

Review

Selecting Catalysts for Pyrolysis of Lignocellulosic Biomass

Maria do Carmo Rangel ^{1,2,*}, Francieli Martins Mayer ^{1,*}, Mateus da Silva Carvalho ^{2,3} , Giovanni Saboia ¹ 
and Arthur Motta de Andrade ¹ 

¹ Institute of Chemistry, Federal University of Rio Grande do Sul, Porto Alegre 90650-001, RS, Brazil

² Institute of Chemistry, Federal University of Bahia, Salvador 40210-630, BA, Brazil

³ Department of Natural and Exact Sciences, State University of Southwest Bahia, Itapetinga 45700-000, BA, Brazil

* Correspondence: maria.rangel@ufrgs.br (M.d.C.R.); francimayer@gmail.com (F.M.M.)

Abstract: The pyrolysis of lignocellulosic biomass is a promising technology for obtaining renewable chemicals and fuels to replace fossil-based products. However, due to the complexity of the lignin, cellulose and hemicellulose molecules, a large variety of compounds are often formed, making commercial implementation difficult. The use of a catalyst during reactions has been recognized as one of the major improvements in pyrolysis, allowing the production of selected compounds. Moreover, the large number of available catalysts opens up a wide range of possibilities for controlling the reaction network. Zeolites, hierarchical zeolites, alkali and alkaline earth oxides, transition metals and carbonaceous materials, among others, have been investigated in the pyrolysis of a variety of biomasses. In addition, bifunctional catalysts play a role in pyrolysis, as well as the addition of plastics as hydrogen donors. This review aims to present and discuss in detail state-of-the-art catalytic pyrolysis, focusing on the relationships between the properties of the catalysts and the obtained products. A guideline for selecting catalysts for lignocellulosic biomass is also provided.

Keywords: pyrolysis; biomass; catalyst; plastics; zeolites; metal oxides; metal salts; activated carbon



Citation: Rangel, M.d.C.; Mayer, F.M.; Carvalho, M.d.S.; Saboia, G.; de Andrade, A.M. Selecting Catalysts for Pyrolysis of Lignocellulosic Biomass. *Biomass* **2023**, *3*, 31–63. <https://doi.org/10.3390/biomass3010003>

Academic Editor: Jaehoon Kim

Received: 27 October 2022

Revised: 29 November 2022

Accepted: 13 December 2022

Published: 10 January 2023



Copyright: © 2023 by the authors. Licensee MDPI, Basel, Switzerland. This article is an open access article distributed under the terms and conditions of the Creative Commons Attribution (CC BY) license (<https://creativecommons.org/licenses/by/4.0/>).

1. Introduction

Since the middle of the last century, mankind has faced several challenges related to the use of fossil fuels. The most critical is to decrease global warming and meet the ever urgently increasing need to supply energy and fuels. In addition, oil and natural gas reserves are not equally located around the world, generating many political and economic conflicts. This scenario has forced most developed countries to look for new sources of energy. These new sources should be investigated and used without damaging the environment and should provide energetic independence. Biomass and lignocellulosic residues greatly fit these requirements, being renewable and widely spread worldwide. Moreover, the development of technologies to produce fuels and chemicals from renewable sources can also generate new jobs and open new markets for the agricultural and forestry sectors. This enables sustainable development and the creation of new products from renewable sources [1]. Another important advantage is the removal of solid wastes from the environment. Currently, biomass accounts for over 50% of the total renewable energy produced in the world [2].

Many technologies are available for converting biomass into fuels and chemicals, such as fractionation, densification, liquefaction, supercritical fluid liquefaction, destructive carbonization, pyrolysis, gasification, hydrothermal liquefaction and hydrothermal upgrading, Fischer–Tropsch synthesis, anaerobic digestion, hydrolysis and fermentation [1–5]. Figure 1 shows the most common methods for biomass conversion [3], the main groups being thermochemical conversion, direct combustion, physical extraction, biochemical conversion, electrochemical conversion and indirect liquefaction. Biochemical conversion involves biodiesel conversion, anaerobic digestion and ethanol synthesis, while indirect liquefaction

includes Fischer-Tropsch synthesis. The thermochemical conversion involves direct liquefaction, pyrolysis and gasification. Among these possibilities, the thermochemical routes have been considered the most feasible ones [3].

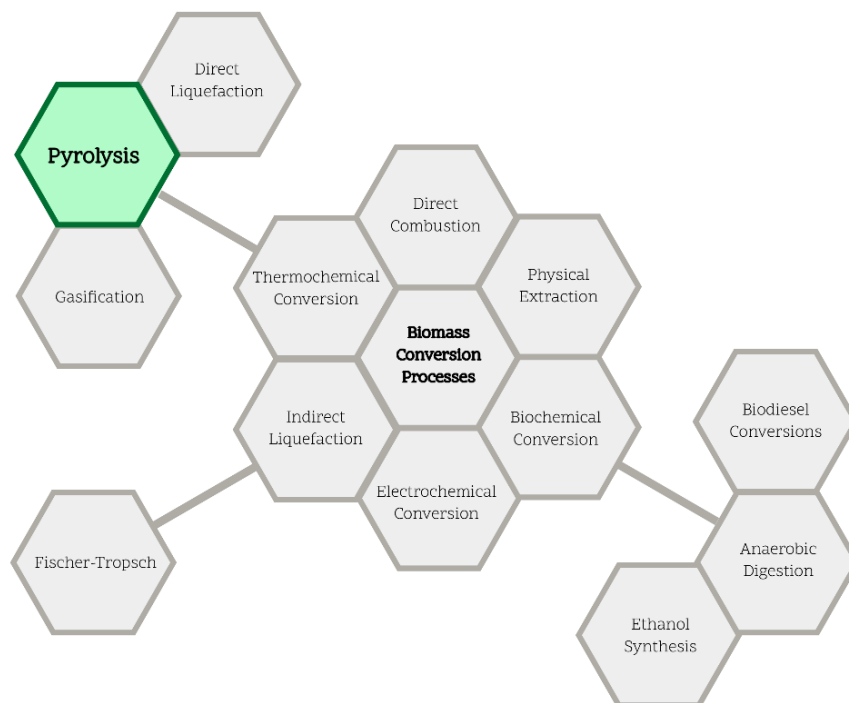


Figure 1. Main methods for biomass conversion. Based on Lin and Waters 2015 [3].

During the liquefaction process, biomass undergoes a complex sequence of physical structure and chemical changes, forming liquefied products consisting of small molecules. They are unstable and reactive, and can repolymerize into oily compounds with a wide range in terms of molecular weight distribution. Liquefaction can be either directly or indirectly performed. In the first case, fast pyrolysis produces liquid tars and oils and/or condensable organic vapors. In the second, non-condensable, gaseous products of pyrolysis or gasification are converted into liquid products over a catalyst [1,3].

During gasification, fossil or non-fossil fuels (solid, liquid or gaseous) are decomposed into useful gasses and chemicals. The process can be carried out in gaseous medium (air, oxygen, subcritical steam or a mixture of them) or in supercritical water [3]. Currently, synthetic gasses are mostly produced from fossil fuels. The process essentially converts a potential fuel to another one to: (i) increase the heating value of the fuel, removing nitrogen and water; (ii) remove sulfur and nitrogen avoiding pollution; and (iii) decrease the carbon-to-hydrogen (C/H) mass ratio in the fuel [5].

On the other hand, pyrolysis is performed in the absence of oxidizing agents or with a limited supply, not allowing biomass gasification to an appreciable extent. Pyrolysis is one of several reactions occurring during gasification [3,5]. In the last few years, pyrolysis has been extensively studied [1–5] and considered as a promising route for producing fuels and chemicals, because of the simplicity, versatility and the possibility of obtaining desirable products in only one step. Pyrolysis has some disadvantages, such as high operational and investment costs. However, it is expected that this drawback can be overcome by the technological development of pyrolysis facilities and the costs of the next generation of power generation equipment. In addition, the use of catalysts can largely improve the low selectivity of this process. Other challenges include finding an economical production for cleaning fuel gasses from biomass pyrolysis [5].

These advantages have motivated many studies to address pyrolysis; lignocellulosic biomass being the most common feed for the process. Biomass is regarded as the non-

fossilized and biodegradable organic material of plants, animals and microorganisms, such as products, byproducts, residues and waste from agriculture, forestry and related industries. The non-fossilized and biodegradable organic fractions of industrial, municipal solid wastes, gasses and liquids recovered from the decomposition of non-fossilized, as well as biodegradable, organic material are also considered as biomass [1]. Among these different types, lignocellulosic biomass is the most studied, especially wood, because of its low ash formation and higher-quality products [2]. Regardless of its origin, lignocellulosic biomass consists of cellulose (40–50%), hemicellulose (25–35%) and lignin (15–20%), in addition to extractives, lipids, proteins, simple sugars, starches, water, hydrocarbons, ash and other compounds [1,4]. However, the amount of each fraction largely depends on the biomass source; for instance, hardwoods have more cellulose, hemicelluloses and extractives than softwoods, but softwoods have more lignin [1]. These molecules are all biopolymers, generating a complex structure with a variable composition, which undergo different reaction pathways during pyrolysis [4].

2. Biomass Pyrolysis

Pyrolysis is an efficient and eco-friendly process, in which biomass (or other feedstock) is heated under an inert atmosphere, usually nitrogen. According to the residence time, pyrolysis can be divided into different classes, which have varied among authors [3,5]. The major categories are: (i) slow pyrolysis, performed at a heating rate of 0.1–1 K/s, with a residence time from minutes to hours and a temperature ranging from 673 to 873 K; and (ii) fast pyrolysis, which is carried out in a range of 673 to 873 K, under heating rates of 10–1000 K/s and with a short residence times (<2 s) [3]. Slow pyrolysis produces mostly char and has been largely used to produce solid fuel for a long period of time [6]. On the other hand, fast pyrolysis of lignocellulose biomass has been highlighted as the most promising route by which to produce sustainable fuels and chemicals. In addition, flash pyrolysis has been proposed, with a shorter residence time (<1 s), high heating rates and at temperatures below 923 K; used to produce bio-oil and gasses [5].

Under pyrolysis conditions, the polymeric structures of cellulose, hemicellulose and lignin continue cracking and produce small gas molecules (carbon monoxide and dioxide, ethene, ethane, propane and others), liquids (tar, heavy hydrocarbons and water) and solids (char), as shown in Figure 2 [7,8]. Using fast heating and quenching, the intermediate liquid products can be collected through condensation, before further reactions break them into gaseous products. At higher fast pyrolysis temperatures, the major product is gas. Pyrolysis can also be performed under small quantities of oxygen (gasification), water (steam gasification) or hydrogen (hydrogenation) [1].

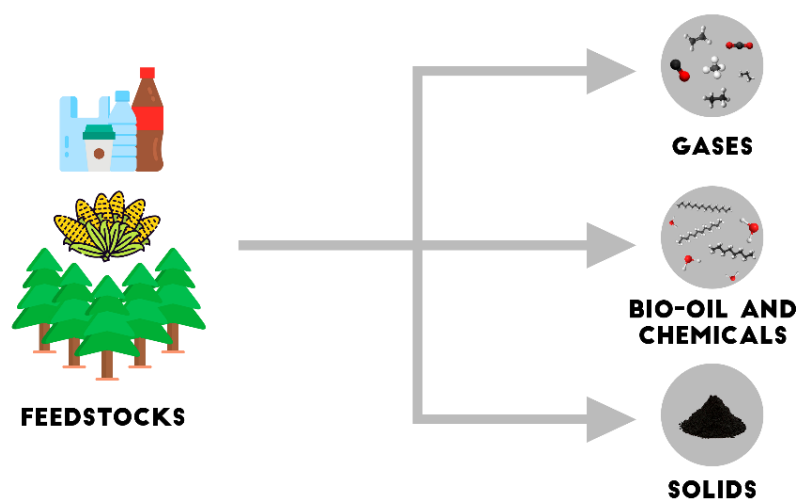


Figure 2. The main products of biomass pyrolysis.

The main interest in fast pyrolysis is the high oil-like liquid fraction (bio-oil) yield (up to 75%) that can be obtained. This fraction is a complex mixture of more than 300 compounds [9], mainly ketones, aldehydes, carboxylic acids, esters, aliphatic and aromatic alcohols and ethers [10]. The most abundant compounds are acetic acid, 1-hydroxy-2-propanone and levoglucosan, coming from cellulose, in addition to several types of phenols, guaiacols, syringols, aldehydes, ketones, carboxylic acids and alcohols from lignin [11]. Because of the large amounts of the reactive oxygenated compounds, bio-oil has undesirable properties, preventing its direct use as a fuel and as feedstock for chemicals production. These properties include: (i) high tendency to polymerize; (ii) low combustion heat; (iii) chemical instability; and (iv) high viscosity and corrosivity [12]. It requires further process steps for upgrading bio-oil by removing the oxygenated compounds to obtain high value-added fuels and chemicals. Several upgrading techniques of bio-oil have been proposed via many methods involving catalysts. They include low temperature esterification with alcohols, catalytic cracking and hydrotreating processes, in addition to hydrodeoxygenation (HDO) [1,2,11].

In a more practical approach, pyrolysis is performed over an appropriated catalyst (direct catalytic pyrolysis) so that the hydrodeoxygenation reaction occurs in situ. Another approach is to carry out catalytic pyrolysis of biomass to produce platform compounds (ketones, furans and others). These compounds react in a further step to produce liquid fuels and high value-added chemicals, such as gasoline and aviation kerosene [13]. Recently, dielectric heating from microwave radiation has also been used for biomass pyrolysis. This process has demonstrated the advantages of providing uniform volumetric heating, energy savings and efficiency, as well as process control flexibility [14].

The composition and distribution of the products of pyrolysis largely depend on temperature, heating rate and residence time. In addition, they are also affected by the kind of atmosphere, biomass and reactor. This requires the optimization of the process conditions for each kind of biomass or each reactor. For instance, Carlson et al. [15], studied the conversion of pine and concluded that the optimized process conditions were 873 K, with a mass space velocity of 0.3 h^{-1} and a catalyst/pine (weight) = 6 to obtain 15.1% of aromatics and 7.8% of olefins.

3. Reaction Pathway during Biomass Pyrolysis

Because of the complex structure of biomass, pyrolysis involves multiple stages of decomposition and multiple reactions, which take place at spatial and temporal scales. After heat transfer begins in the vertical direction of the cell cavity of biomass, free moisture evaporates, followed by primary decomposition and secondary reactions, like oil cracking and re-polymerization [16,17]. In the first step (primary decomposition), cellulose undergoes decomposition in a range of 473 to 673 K, producing char. Meanwhile, hemicellulose begins to decompose at 523 up to 623 K to produce xylan. From 598 to 673 K, cellulose (also side reactions) produces levoglucosan and furan [18], which decompose into light oxygenates and furanic species at higher temperatures. Lignin undergoes decomposition at a wider range of temperatures (433 to 1173 K), with monolignols being produced at lower temperatures, and phenols and light oxygenates at higher temperatures. Other secondary reactions also take place in the solid biomass with increasing temperatures [19]. As cellulose, hemicellulose and lignin are constituents of biomass, their decomposition simultaneously occurs in certain ranges of temperature.

The main reactions of pyrolysis include deoxygenation, aromatization, ketylation, alcohol aldehyde condensation and catalytic cracking [20]. They selectively occur, depending on the catalyst and on the process variables, so that the lignocellulose structure can produce high quality bio-oil or chemicals. Aromatics production from a lignocellulosic biomass over a zeolite catalyst, for instance, is shown in Figure 3. As we can see, pyrolysis involves a complex network of reactions, coming from the decomposition of hemicellulose, cellulose and lignin. Most steps involve oxygen removal, producing water (by dehydration), carbon monoxide (by decarbonylation) and carbon dioxide (by decarboxylation), illustrating the

role of the catalysts in promoting these reactions. The main initial products are anhydro-sugars and furan compounds, from cellulose and hemicellulose decomposition on the acid sites of catalysts by the dehydration of cellulose. It is followed by the production of furanic species (furan, methylfuran, furfural), small aldehydes and water through dehydration, bond cleavage and bond rearrangement in the gas phase. In the next step, hydrocarbons and carbon monoxide are produced by oligomerization, decarboxylation, decarbonylation and dehydration reactions of furan compounds over the zeolite catalyst [21]. Furthermore, aromatic molecules of lignin undergo depolymerization, producing olefins over the catalyst. The phenolic compounds undergo cracking and H-transfer reactions on the acid sites of zeolite, leading to benzene, toluene and xylene [22]. Polymerization and isomerization can also occur during pyrolysis of lignocellulosic biomass [23].

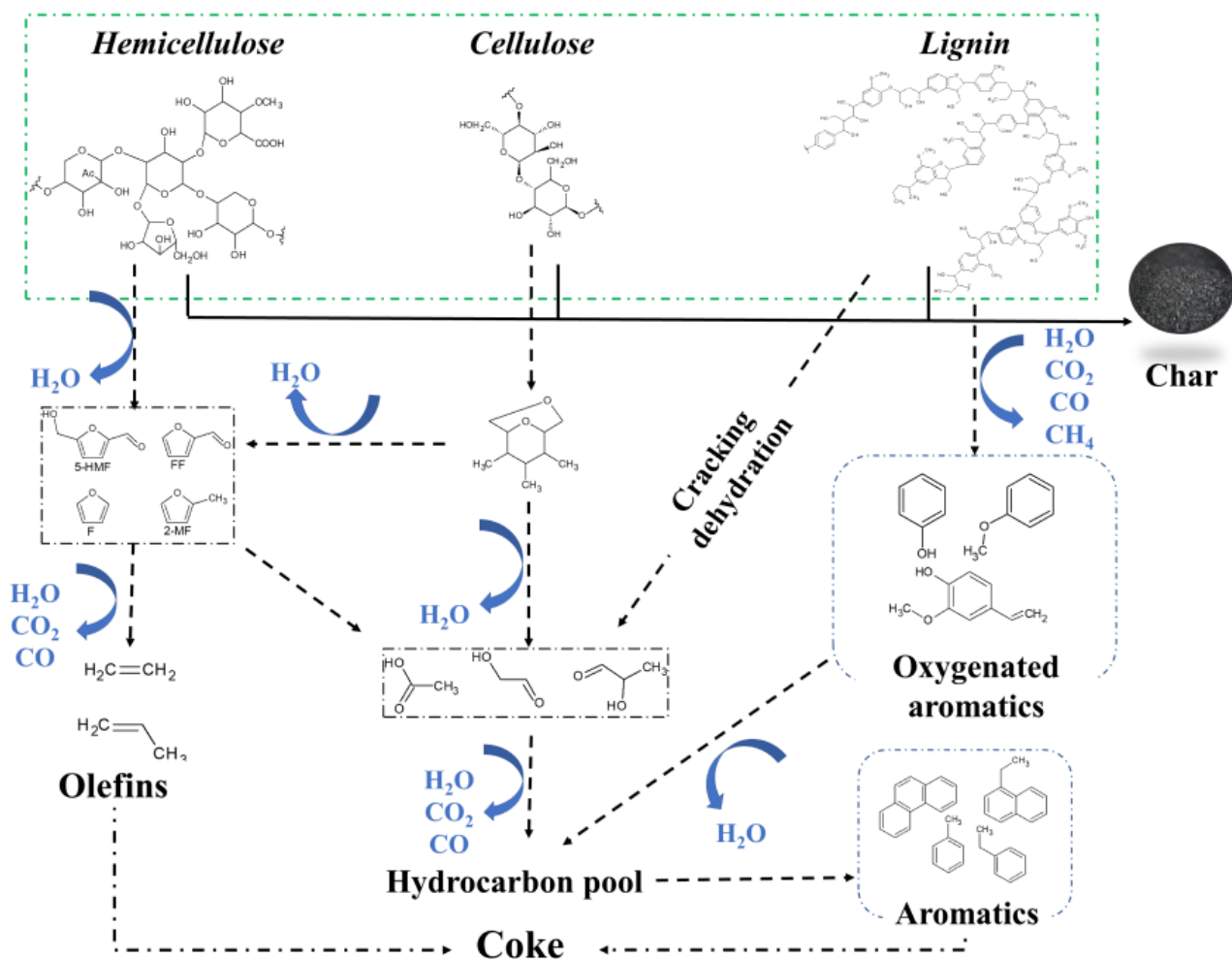


Figure 3. Reaction pathways of biomass pyrolysis over a zeolite. Based on Wang et al. 2022 [16].

4. Catalytic Pyrolysis of Biomass

Catalytic pyrolysis can be performed by two experimental arrangements, so-called in situ and ex situ pyrolysis, as illustrated in Figure 4. In the first case, the feedstock and catalyst are previously mixed and then introduced into the reactor, where the upgrading of solid and vapor phases simultaneously occurs [24]. In this arrangement, biomass and catalyst particles come into contact in the fluidized bed, favoring biomass decomposition. In addition, the large molecules produced by the primary decomposition of biomass will contact the catalyst more easily and then will react faster [13,16]. The vapors diffuse into catalyst pores, where they undergo cracking and other reactions [23]. This increases the pyrolysis degree and decreases the probability of the further reaction of pyrolysis

products [13]. This configuration has some drawbacks, such as the pyrolysis temperature, which cannot be optimized for catalyst activation, and the possibility of some vapors not entering into the catalyst pores before attaining the reaction temperature [25]. In addition, high coke can be produced on the catalyst, decreasing both bio-oil yields and quality [26].

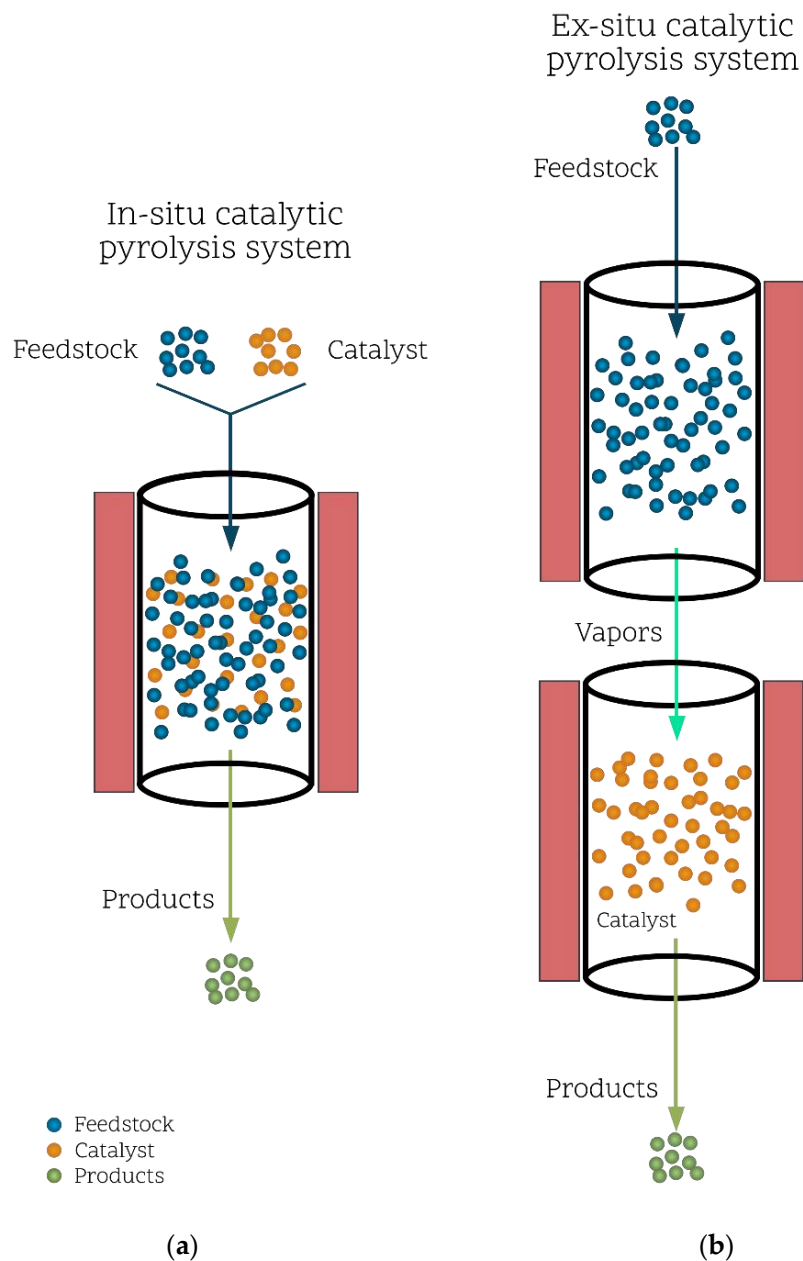


Figure 4. (a) In situ and (b) ex situ configurations of catalytic pyrolysis of biomass.

For both cases, the reusability of the catalysts has been scarcely investigated. Some studies have been recently reported [27–29] concerning the reusability of catalysts for ex situ pyrolysis. However, the reusability of catalysts used in in situ configurations has an additional difficulty related to the recovery of the catalysts from char. A possibility for overcoming this drawback is the use of magnetic particles as catalysts.

In ex situ pyrolysis, the feedstock is introduced into the reactor and biomass is cracked to produce pyrolytic vapors which pass over a catalytic bed, where the upgrading is carried out, forming bio-oil, gaseous products and solid by-products. This process has the advantage of cracking and pyrolysis temperatures that can be independently adjusted to optimize maximum catalytic activity under optimum conditions [30]. Furthermore, the

char produced can be used to produce heat energy, but longer vapor residence leads to further secondary reactions, producing water and coke. However, the requirement of an additional catalytic reactor is a cost-related limitation. Compared to the in situ process, it leads to higher selectivity for aromatics and syngas [16].

For both cases, the amount and distribution of the products depend on the catalyst type and the catalyst-to-biomass ratio, in addition to the process variables such as temperature, reactor type, biomass particle size, heating rate and residence time [24]. Regardless of the mode of operation, the amounts of catalyst and biomass are fed into the reactor according to the chosen value of the catalyst-to-biomass ratio. For continuous operations, the biomass and catalysts are continuously fed into the reactor, maintaining the chosen value of the catalyst-to-biomass ratio.

In addition to the significant improvement in quality and yield of bio-oil and the increase of different aromatic hydrocarbons [16], the catalyst increases the yields of five main petrochemical products: toluene, benzene, ethylene, propylene and xylene [24]. To maximize aromatic yields, proper catalysts (considering pore structure and active sites) should be used [31]. In addition, high catalyst/biomass and heating rates are needed to guarantee the diffusion of volatile organic compounds into the catalyst pore prior to decomposition into coke [32]. The bio-oil produced by catalytic pyrolysis is deeply deoxygenated, resulting in a high hydrogen-to-carbon (H/C) ratio [33]. The lower amount of oxygen minimizes the number of acidic components and decreases the corrosive nature of the bio-oil [32]. Furthermore, the production of char can be decreased by the catalyst, increasing bio-oil stability [23,34].

All the desired products can be tailored by the appropriate selection of the catalyst. In addition, the operation can be performed in one step and at short residence times (less than 10 s), minimizing secondary reactions. Other advantages of pyrolysis include: the use of an inert atmosphere (avoiding high-pressure hydrogen); no need of using water; the need for only simple pretreatment processes for the feedstock (grinding and drying) and the possibility of using inexpensive catalysts, such as alumina and silica [23].

As expected, the catalysts decrease the activation energy, and then, the pyrolysis temperature, providing more favorable energetic reaction pathways [35]. This reduces equipment and energy costs and increases biomass conversion, in addition to the possibility of tailoring the distribution of products by different catalysts [23]. Therefore, in situ catalytic pyrolysis is the simplest and most economical route for performing biomass pyrolysis.

5. Properties of the Catalysts for Biomass Pyrolysis

Because biomass has a complex chemical structure with varied components in multiple forms, in addition to the process variables of pyrolysis, numerous catalysts and additives are required to achieve the desired upgrading of bio-oil and chemical production.

Since biomass pyrolysis involves multiple reaction pathways, different catalysts will change the activation energy and the rate of each reaction in different ways. Different catalytic reactions occur on the metal and/or on acidic/basic sites by redox or H-transfer mechanisms, respectively. Some reactions require the cooperation of metallic and acidic sites, generating bifunctional catalysts. They include ring-opening in double or more rings in two stages. Firstly, aromatic rings are hydrogenated on the metal and then form tetralin and derivatives which continue cracking to produce monoaromatics over the acidic sites [36]. Other reactions require both acidic and basic sites, which cooperatively act [37]. It has been found, for instance, that the dehydration, depolymerization, C-C or C-O cleavage and ring-opening reactions are favored by high acidity/basicity ratio [38].

Therefore, the catalysts can be designed to focus the desired products, based on their diverse properties, such as strength and the distribution of Brønsted and Lewis acid (or basic) sites, porosity and following the addition of a metal. Moreover, the pore size and distribution, specific surface area, and the phases and structure of the catalysts should also be considered in its design. These properties can impact the activity and selectivity and, subsequently, the yield of desired products.

In addition to the properties of the catalysts, the pyrolysis feedstock can widely vary, requiring catalysts with different functionalities, which should be designed for each kind of biomass, focusing on the desired products. Furthermore, like most industrial catalysts, the solids for catalyzing biomass pyrolysis for commercial purposes should show high resistance against deactivation and have recycling ability and low costs, in addition to high activity and selectivity [39].

5.1. Specific Surface Area and Porosity

This property is one of the most fundamental of solid catalysts for their use in heterogeneous reactions, in both liquid and gas phases. It is believed that a high specific surface area will provide efficient contact between the reactant molecules and the active sites. In addition, the high specific surface area of the support will favor the high dispersion of metal, forming small and highly active particles. Therefore, high specific surface areas are required for almost all heterogeneous reactions, including pyrolysis.

5.1.1. Oxides and Other Microporous Solids

For metallic oxides, such as iron oxide, aluminum oxide, magnesium oxide and zirconium oxide, among others, their specific surface areas are in a range of 20–200 m² g⁻¹ [40–42]. These solids are typically macroporous, and these values are basically related to particle sizes. Over them, the catalytic reactions, including pyrolysis, will occur on the external surface, since they have no pores. Therefore, high surface areas are always required so that voluminous molecules can achieve active sites, without steric hindrance, due to the large amounts of these molecules on the surface [43,44].

5.1.2. Zeolites and Mesoporous Materials

The disadvantage of steric hindrance, due to the large amounts of voluminous molecules on the external surface, can be overcome by performing pyrolysis over highly porous materials, such as zeolites (microporous) and mesoporous materials. In these cases, the porous structure is quite important, since the pore dimensions, instead of the size of particles, determine the specific surface area. For these materials, the specific surface areas can achieve 1000–2000 m² g⁻¹ thanks to micropores and mesopores [45,46]. However, most of the active sites are located inside the pores, requiring the diffusion of reactant molecules to the pores.

This access will be determined by the pore sizes, which regulate the entrance of reactant molecules into the pores and then to the active sites. Such a situation has been noted by several authors using HZSM-5 (Zeolite Socony Mobil—five) and other zeolites. Stefanidis et al. [43], for instance, studied the effect of ZSM-5 catalysts on upgrading biomass vapors and found that increasing the specific surface area of the catalyst increased the quality of bio-oil, this being accompanied by a low number of undesirable by-products.

For aromatic fraction in bio-oil, the pore size of zeolites determines the bio-oil production. It has been noted [47] that micropores limit the diffusion of the reactant molecules into the active sites, producing a mixture of oxygenates, coke and syngas, instead of aromatics. Furthermore, a fast deactivation by pore blockages on the zeolite surface was observed. On the other hand, zeolites with large pores, such as beta zeolite (~6 × ~7 Å), produce more polyaromatic hydrocarbon (PAH) than monoaromatic hydrocarbon (MAH) in the pores. This is related to the space inside the large pores, being big enough to allow the diffusion of primary products and to favor the formation of PAH molecules. However, PAH are undesirable compounds as they act as coke precursors [48]. Lin et al. [49] compared four zeolites with different pore sizes (HZSM-5, HBeta, HY and HUSY), and highlighted that a zeolite with a medium pore size can modulate the aromatic production by shape selectivity, resulting in high yields of aromatics and hindering coke formation. On studying the catalytic fast pyrolysis of kraft lignin over conventional, mesoporous and nanosized ZSM-5, Lazaridis et al. [50] found that, over HY and HBeta (larger pore size), PAHs (tri-, tetra-, methylbenzenes and methylnaphthalenes) were the main products. On the other hand,

over HZSM-5 (smaller pore size), MAH (toluene and naphthalene) were preferentially produced. In addition, the nano-sized and mesoporous ZSM-5 (prepared by treating ZSM-5 with a mild alkaline solution) were highly selective in the production of (alkyl)phenols. On the other hand, the nano-sized ZSM-5 zeolite produced the lowest amount of bio-oil and the highest production of water, coke and non-condensable gasses, compared to the conventional microporous and mesoporous ZSM-5 zeolite. These differences were most related to pore size rather than to the acidity of zeolites.

Zeolites can be classified into three main groups, considering the pore system. The first class includes those with small pores, formed by 8-membered oxygen rings (3 to 4.5 Å) and interlinked supercages (large cavities formed at the intersection of multiple channels). They hinder coke formation and catalyst deactivation. Zeolite A and ZSM-34 (Zeolite Socony Mobil—thirty-four) are included in this group, as shown in Figure 5. The second class has medium pores formed by 10-membered oxygen rings (4.5 to 6 Å), such as ZSM-5 and ZSM-11 (Zeolite Socony Mobil—eleven). The third class has dual pore systems with 8- and 10-membered oxygen ring openings or 8- and 12-membered oxygen ring openings (6 to 8 Å), such as mordenite (MOR), X zeolite, Y zeolite, beta zeolite and stilbite [51].



Figure 5. Classification of zeolites according to the pore system. Medium pore zeolites: MEL (Zeolite Socony Mobil-eleven, ZSM-11) and MFI (Zeolite Socony Mobil-five, ZSM-5). Dual pore system zeolites: BEA (Zeolite Beta polymorph A) and MOR (Mordenite). Small pore zeolites: LTA (Linde Type A), Zeolite A, OFF (Offretite) and ZSM-34 (Zeolite Socony Mobil-thirty-four).

Therefore, shape selectivity (an intrinsic property generated by zeolitic structure) can be used to tailor the desired product, since the oxygenated lignin derivatives are bulky molecules. Yu et al. [52] compared the x, y and z dimensions of the pore openings of ZSM-5, mordenite, beta and Y zeolites in the protonic forms, to evaluate which oxygenated molecules derived from lignin could access the inner surface of them. They observed that the z-dimension of all lignin-derived oxygenates were smaller than the diameter (conjugated) of the zeolite pores (except for the pore with eight rings of mordenite). This indicated the dependence on the y-dimension associated with the diameter (transversal) of the pore openings of zeolites. All lignin-derived oxygenates (except furfural and phenol) could not enter the pores of ZSM-5 and mordenite. Furthermore, a comparatively small fraction of these oxygenates could enter the pores of beta and Y zeolites. These results

indicate that most oxygenates can only be converted at the external surface, where catalysts contain only a small fraction of sites [52].

To overcome this limitation, hierarchical zeolites have emerged as promising alternatives for biomass pyrolysis, by combining catalytic activity with an accessible pore structure, as shown by several authors. Kim et al. [53], for instance, investigated the pyrolysis of woody polymer composites over hierarchical ZSM-5 and beta zeolite (Figure 5). A substantial increase in aromatics production was noted, as compared to non-catalytic pyrolysis. Over zeolites, wood was initially decomposed into oxygenates, which then diffused into the pores, where they reacted through dehydration, dealkylation, dealkoxylation, decarbonylation and decarboxylation reactions over acidic sites inside the pores. Light hydrocarbons, furans, ketones and phenols were obtained as final products. Acidic beta zeolite led to the highest conversion of bulky molecules in the products, in addition to producing the lowest number of aromatics. Furthermore, it produced a higher relative quantity of linear and branched hydrocarbons than the other catalysts, suggesting higher cracking activity, more efficient mass transfer and a higher number of acid sites than ZSM-5. As compared to beta zeolite, the acidic form produced higher amounts of aromatic hydrocarbons due to its higher mesoporosity and acidity [53]. The combination of micro- and mesoporosity reduced the tendency to sinter and to produce large metallic nanoparticles [54]. Qian et al. [55] compared the production of aromatic hydrocarbons over mesoporous ZSM-5 modified with nanocellulose to conventional and alkali-treated mesoporous ZSM-5. The hierarchical ZSM-5 showed higher selectivity to MAH and a decrease in coke accumulation. They noted an increase in the specific surface area of modified mesoporous ZSM-5 ($118.8 \text{ m}^2 \text{ g}^{-1}$) in comparison to a conventional ZSM-5 ($75.0 \text{ m}^2 \text{ g}^{-1}$) one. This caused an increase in deoxygenation, and then, of MAH and bio-oil. Therefore, the overall efficiency of aromatic hydrocarbon formation from biomass via catalytic pyrolysis can be controlled by the rate of mass transfer to the active sites of the catalyst through shape selectivity [53].

Mesoporous materials have also been used for biomass pyrolysis, mainly because of their high porosity and specific surface areas. Casoni et al. [56], for instance, studied the pyrolysis of cellulose over MCM-41, Al-MCM-41, Fe-MCM-41, Al-Fe-MCM-41 and Cu-MCM-41, noting an increase in liquid products. This was related to the acidity of the catalysts, which promoted dehydration reactions, lowering the levoglucosan production, while increasing the other anhydrosugars.

5.1.3. Carbonaceous Materials

Carbon is one of the most abundant elements on Earth's surface and can be found in assorted forms. Charcoal, biochar and activated carbon are amorphous carbons. Charcoal produced by the thermochemical chemical conversion of feedstock can be modified by activation processes to yield activated carbon. Sourcing the organic feedstock from sustainable and renewable origins produces biochar, eco-friendly charcoal used as a starting material for activated carbon. These solids are typically microporous, but some mesoporous carbons can also be found [57]. The morphology and physical-chemical properties of obtained carbonaceous materials significantly vary. However, these properties can be modified by assorted chemical activation processes [58–60]. Understanding the impact of the different properties of the catalysts prepared with these new carbonaceous materials on the catalytic pyrolysis of lignocellulosic biomass is vital to designing new catalysts for targeted results.

The morphology and pore system of the catalysts are important factors for catalyst activity [61–65]. Figure 6 shows different pore structures of carbonaceous solids and some surface functional groups [66]. Because of their high specific surface area and pore volume, they are expected to exhibit high catalytic activity thanks to the augmented amount of available active sites on the surface and in the pores [61,63,65]. In addition, the porous structures allow for the diffusion and further upgrading of pyrolytic vapors into the pores [66]. Hence, a catalyst with a high specific surface area and high porosity will favor the cracking of pyrolytic intermediates and the formation of gaseous products [61].

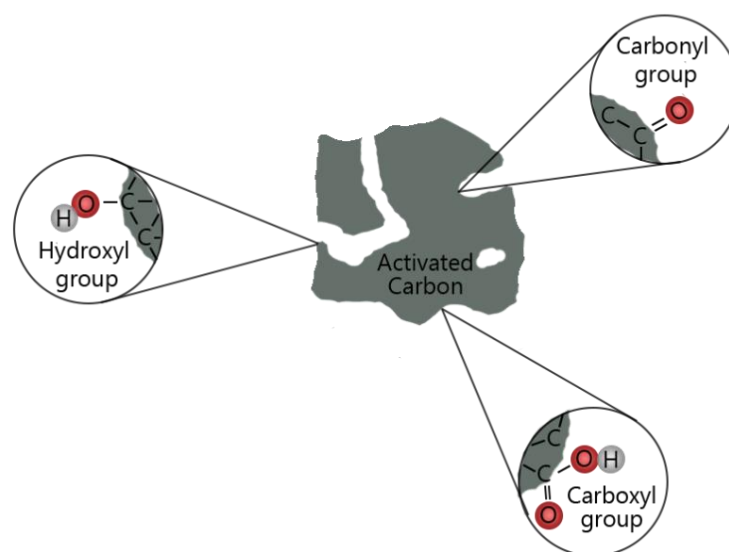


Figure 6. An illustration of hydroxyl, carbonyl and carboxyl groups on the surface of a carbonaceous solid.

These materials have been extensively studied for biomass pyrolysis in recent times, because of the need for economical and greener processes for cellulose conversion. Carbonaceous materials are stable in different media and can be used in pre-treatments, reactions and other operations performed in water, organic solvents or ionic liquids [51,67]. For some applications, they are prepared by an incomplete carbonization of biomass to obtain amorphous carbons [60], followed by sulfonation using concentrated sulfuric acid and chlorosulfonic acid [51,68]. The sulfonation leads to the production of phenolic hydroxyl ($-OH$), carboxylic ($-COOH$) (Figure 6), and sulfonic (SO_3H) groups; the former two groups having ability to adsorb cellulose by van der Waals forces, and to break the intermolecular and intramolecular hydrogen bonds of cellulose [51,69]. These groups also act as hydrolyzing agents, resulting in high activity [51]. Table 1 presents some examples of activated carbon-catalytic pyrolysis studies performed in the last decade.

Table 1. Activated carbon catalysts applied to catalytic pyrolysis of biomass.

Feedstock	Catalyst	Pyrolysis System	Operational Conditions *	Main Products	Ref.
Douglas Fir sawdust pellet	Commercial acid-washed steam-activated carbon	Microwave-assisted reactor (power 1 kW, frequency 2450 MHz)	673 K 8 min 1:3 NA **	Phenols	[70]
Peanut shell Pine sawdust	Activated carbon	Microwave-assisted reactor (power 2 kW, frequency 2450 MHz)	573–873 K 50 min 8:1 and 8:2 N_2 400 mL·min ⁻¹	Phenols	[71]
Palm kernel shell	Activated carbon	Fixed-bed reactor	673–873 K 40 min 3:0.5 and 3:1 N_2 1000 mL·min ⁻¹	Phenols	[72]
		Microwave-assisted reactor (power 2 kW, frequency 2450 MHz)	673–873 K NA ** 10:1 and 10:2 N_2 400 mL·min ⁻¹		

Table 1. Cont.

Feedstock	Catalyst	Pyrolysis System	Operational Conditions *	Main Products	Ref.
Sugar cane bagasse Poplar wood Pine wood	H ₃ PO ₄ -activated carbon H ₂ O-activated carbon CO ₂ -activated carbon ZnCl ₂ -activated carbon	Py-GC/MS	523–773 K 20 s 1:0, 10:1, 5:1, 3:1, 2:1, 1:1 and 1:2 NA **	Levogluosenone	[73]
Bamboo wastes Spirulina platensis	Biochar	Fixed-bed reactor	873 K 10 min 2:1 Ar 200 mL·min ⁻¹	Aromatic Hydrocarbons Phenols	[74]
Corn sotver	H ₃ PO ₄ -activated carbon	Fixed-bed reactor	702–843 K 8 min NA ** N ₂ 100 mL·min ⁻¹	Phenols Syngas	[75]
Rice husk Corn cob	Fe-supported biochar	Microwave-assisted reactor (power 1 kW, frequency 2450 MHz)	773 K 20 min 1:1 (ex-situ) Under vacuum	Phenols	[62]
Bamboo waste	N-doped biochar	Fixed-bed reactor	873 K 30 min 2:1 Ar 200 mL·min ⁻¹	Phenols	[76]
Douglas Fir	H ₃ PO ₄ -activated carbon impregnated with MgO	Fixed-bed reactor	673–873 K 15 min 1:0, 2:1, 1:1 and 1:2 N ₂ 60 mL·min ⁻¹	Phenols Furans Aldehydes Ketones	[64]
Bamboo waste	KOH-activated biochar K ₂ CO ₃ -activated biochar KHCO ₃ -activated biochar CH ₃ COOK-activated biochar	Fixed-bed reactor	873 K 30 min 2:1 (ex-situ) Ar 200 mL·min ⁻¹	Aromatic Hydrocarbons Phenols	[61]
<i>Chlorella vulgaris</i>	Acid-washed biochar KOH-activated carbon Fe acid-washed biochar Fe KOH-activated carbon	Dual-bed reactor	723–1123 K 30 min 2:1 (ex-situ) Ar 30 mL·min ⁻¹	Hydrocarbons Phenols Acids Alcohols	[77]
Pine sawdust	CO ₂ -activated carbon	Fixed-bed reactor	873 K 10 min 2:5 (ex-situ) NA **	Phenols	[63]

* Operational conditions: temperature, residence time, feedstock to catalyst ratio and gas flow ** NA: not available.

5.2. Acidic and Basic Sites

Because the acidic or basic sites are essential for the suitable catalytic performance in biomass pyrolysis, the catalysts are often classified into acidic (zeolites, metal oxides and acidic carbons) and basic (alkali metal oxides, alkaline earth metal oxides, salt metals and basic carbons) catalysts [51]. However, this classification is not rigid, as several compounds can act both as acids and as bases.

5.2.1. Acidic and Basic Zeolites

Zeolites are important microporous crystalline materials formed by the linkage of TO₄ tetrahedra (T = Si or Al) in different ways, resulting in 253 types of framework topologies. The empirical composition of zeolites can be represented by the formula: Mⁿ/x[(AlO₂)x(SiO)y]·wH₂O, where M = exchangeable cation; n = valence of the cation;

$(x + y)$ = total number of tetrahedra per unit cell and w = number of water molecules [78]. The structures of zeolites can vary, as illustrated in Figure 5, and their connectivity can also vary due to the cages within the channel, in addition to the possible formation of one-dimensional, two-dimensional and three-dimensional channels [79]. Due to their great versatility, zeolites are used in many relevant industrial processes, such as adsorption [80], separation [81] and catalysis [82–84].

The catalytic applications of zeolites are largely related to the intrinsic acidity of Brønsted and Lewis, originating from their peculiar structure. The acidity in zeolite comes from the introduction of trivalent aluminum ions into the structure, generating delocalized charges throughout the material, as shown on the right of Figure 7. This charge is counterbalanced by cationic species, leading to the creation of Brønsted acid sites, shown on the left of Figure 6. These sites are catalytically active and donate an acidic proton to pyrolytic substrates (oxygenate and hydrocarbon), leading to carbocation intermediates which are converted to olefins through the β -scission process [79]. Brønsted acidity is usually the most important in the fine chemical industry and in oil refining [82–84]. The isomorphous substitution of silicon for aluminum in the tetrahedron gives the aluminosilicates Lewis acidity (or non-protonic acidity) [85]. These properties make zeolites suitable materials for catalyzing biomass pyrolysis, the main motivation being the acidic nature which facilitates the breaking of the C-C and C-O bonds. However, polymerization can also occur [86], leading to coke formation, and thus, to catalyst deactivation.

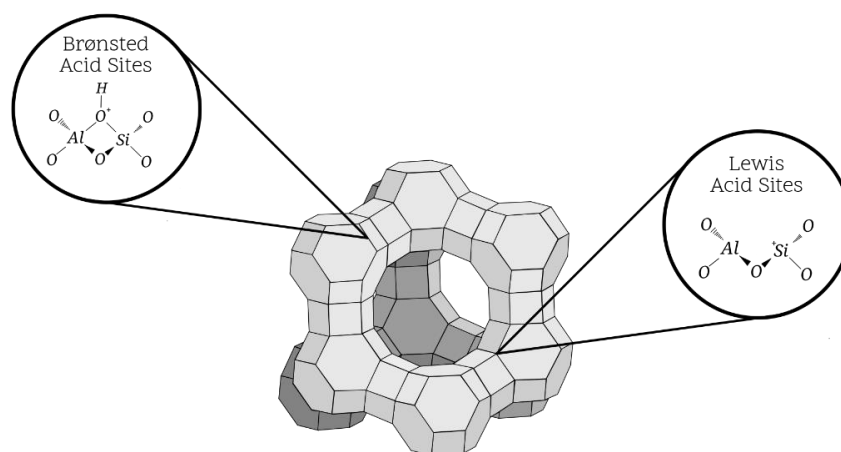


Figure 7. Generation of acidity in zeolites. The Lewis acid sites are generated by the non-balancing and dislocated charges due to the replacement of silicon by aluminum ions. The Brønsted acid sites are created by the counterbalancing of charge by cationic species.

Several zeolites (HZSM-5, Y zeolite, MCM-41, SBA-15, beta zeolite and others) have been used in pyrolysis of biomass to obtain chemicals or fuels [13,87–89]. High value-added species such as furans and aromatics were produced, promoted by the acid sites which act on the decomposition of phenolics. In addition, Mayer et al. [90] noted that the pyrolysis of MDF (medium density fiber) residues over HZSM-5 resulted in the production of 37.91% of monoaromatics, such as BTX (benzene, toluene and xylenes) and others, compared to the non-detectable amount without any catalyst under the same conditions. This behavior was associated with the ability of acidic sites in HZSM-5 to promote deoxygenation reactions, removing oxygen [90]. Different results were obtained by Jin et al. [91] during lignin pyrolysis, where about 75 wt% of phenolics, and less than 5 wt% of aromatic hydrocarbons were detected. However, over HZSM-5, several upgrading reactions occurred, such as deoxidation and polymerization, resulting in a higher proportion of monoaromatic and polyaromatic hydrocarbons [91]. Therefore, the high acidity of the catalysts favored deoxygenation reactions, decreasing the amount of phenolics and increasing the number of hydrocarbons. These studies have shown the potential of HZSM-5 for biomass pyrolysis.

In addition to its activity in deoxygenation reactions, it has hydrothermal stability, acid strength and density [92].

Beta zeolite is another convenient option for biomass pyrolysis, due to the high acidity and selectivity in deoxygenation reactions, in addition to its larger pores, compared to HZSM-5. Mayer et al. [36] evaluated the performance of beta zeolite in the pyrolysis of MDF to produce BTX. Beta zeolite has wide pores ($\sim 6 \text{ \AA} \times \sim 7 \text{ \AA}$), which facilitate the diffusion of the products of primary thermal degradation of biomass, improving the conversion and stability of the catalyst. Among the catalysts, beta zeolite was more active in removing the oxygen from pyrolytic vapors of pre-treated MDF (99%), and in the production of aromatic hydrocarbons (AH). However, high amounts of toxic PAH, such as benzo(a)pyrene, dibenz(a,h)anthracene, naphthalene, benzo(a)anthracene and chrysene, with potential carcinogenic, mutagenic and teratogenic activities [93], were also produced. This is related to the large pores of beta zeolite, which allow the diffusion of primary products, and then, PAH are produced on acidic sites. This problem was overcome by introducing nickel, resulting in a bifunctional catalyst, which hindered the PAH production and increased the selectivity towards BTEX (benzene, toluene, ethylbenzene and xylenes). The decrease in PAH production was related to the cooperative action of metallic sites from nickel and acid sites of beta zeolite, which is efficient in multi-ring-opening reactions, decreasing the PAH content. Due to the ability of nickel to hydrogenate, it breaks the PAH molecules, forming tetralin or its derivatives. In the second step, these molecules undergo cracking over acid sites. In addition, the efficiency of the nickel catalysts was associated with the aluminum chemical environments, which were changed, altering the activity, the amount and the strength of acid sites. The increased BTEX production was assigned to the increased activity in cracking/hydrocracking, hydrogenation/dehydrogenation and isomerization producing aromatics over the stronger sites. For these catalysts, the number of oxygenated compounds increased, indicating lower activity of these catalysts in the reactions related to oxygen removal, mainly HDO and deoxygenation. This finding was related to the decrease in Brønsted sites due to nickel incorporation.

For hierarchical zeolites, nickel loading also affects selectivity. Beta zeolite loaded with nickel, for instance, led to high selectivity toward gasoline range products. However, the increase in activity depends on zeolites, as observed by Escola et al. [94]. They detected a substantial reduction in olefin conversion when hierarchical Ni/ZSM-5, instead of Ni/beta zeolite was used, which was assigned to an insufficient balance between acid and metal functions [94]. In another work, Dai et al. [95] reported that, in the pyrolysis of torrefied corn on the cob over a Ni-modified hierarchical ZSM-5 catalyst, activation energy was decreased for nickel-based catalysts. Furthermore, higher yields of aromatic hydrocarbons were produced, although the acidity of the catalyst decreased [95].

Zeolites modified with a basic component can also be used in biomass pyrolysis. Hernando et al. [96], for instance, found that the addition of magnesium and zinc to ZSM-5 and beta hierarchical zeolites increased bio-oil yield and the degree of deoxygenation, in addition to decreasing coke formation.

In general, the use of a basic catalyst leads to a decrease in oxygenates and acidic compounds in bio-oil produced from catalytic pyrolysis, improving its quality. Although basic catalysts are not efficient for C-C bond cleavage, basic site selectivity favored double bond migration, and then, C-C bond cleavage is facilitated during deoxygenation reactions [97]. Furthermore, basic catalysts are more selective to deoxygenation than their acidic counterparts. Basic catalysts are very resistant to deactivation by coke, since it promotes the continuous removal of oxygen as water and carbon oxides, in addition to the large pores of zeolites [98]. Moreover, previous studies have shown that basic catalysts are able to convert acidic fractions, such as carboxylic acid, into hydrocarbons through decarboxylation [99].

5.2.2. Acidic and Basic Metal Oxide Catalysts

No simple trend has been noted for the behavior of acidic metal oxides (alumina, silica and alumina-silica) in biomass pyrolysis. The strength and quantity of acidic sites can

lead to the selectivity of aromatic compounds, anhydrosugars and furans [13,100–102]. In general, the use of acidic metal oxide alters the distribution of the liquid product, while decreasing its yield. In addition, solid and gas yields can be increased. Chen et al. [103] compared the balance between the yield and quality of bio-oil produced during catalytic pyrolysis of cotton stalks using a fixed-bed reactor. The bio-oil quality was measured by acidity, resistance against corrosivity, aging and viscosity in a similar way to diesel [104]. The balance between yield and bio-oil quality can be determined by improving bio-oil quality with the smallest decrease in bio-oil yield [103].

Acidic (alumina), basic (calcium oxide and magnesium oxide), transition (copper oxide, iron oxide, nickel oxide, zinc oxide and titania) metal oxide, HZSM-5 and MCM-41 were compared. Alumina showed a more pronounced increase in gas phase yield compared to the other catalysts. The composition of the gas phase was also changed; carbon dioxide content was reduced, while carbon monoxide increased. This behavior was related to decarbonization reactions. Alumina, HZSM-5 and MCM-41 showed the best performance in bio-oil deoxygenation, but alumina showed the best balance between bio-oil yield and quality, along with calcium oxide and nickel oxide. These three catalysts (alumina, calcium oxide and nickel oxide) produced the lowest removal of oxygen as water, when compared to the others, suggesting that dehydration was not favored by the balance between yield and bio-oil quality [103]. Therefore, these catalysts were the least efficient in removing oxygen among the studied catalysts.

Metal oxides have been used in both in situ and ex situ pyrolysis of biomass, aiming to selectively obtain high-added value in chemicals for industry, such as phenolic compounds, ketones and furans [101]. Table 2 shows some examples of these systems.

Table 2. Some examples of metal oxide and metal salt catalysts for biomass pyrolysis.

Catalysts	Biomass	Reactor	Main Results	Ref.
CaO and HZSM-5	Waste mixed cloth	Py-GC/MS	CaO increased ketones, aliphatic HC and aromatics.	[105]
CaO	Cotton stalk	Fixed-bed reactor	Increased furans. Decreased carboxylic acids.	[101]
CaO, MgO and ZnO	Palm empty fruit bunches	Fixed-bed reactor	CaO promoted deacidification. MgO decreased levoglucosan. Catalysts increased water in the bio-oil.	[106]
CaO and MgO	Forest residues	Batch tubular reactor	CaO showed better deoxygenation power than MgO, and increased H ₂ content and CO ₂ absorption.	[107]
CaO	Oakwood	Py-GC/MS	Increased ketones and light phenols. Decreased carboxylic acids, furans, and heavy phenols.	[108]
CaO, Ca(OH) ₂ and Ca(COOH) ₂	Switchgrass	Fluidized bed reactor	Decreased acetic acid and levoglucosan. Increased phenols and HC.	[109]
CoO, Cr ₂ O ₃ , CuO, Fe ₂ O ₃ , Mn ₂ O ₃ , NiO, TiO ₂ , V ₂ O ₅ and CeO ₂	Poplar wood	Fixed-bed reactor	Catalysts promoted alcohol, furans, ketones, acetic acid and phenolic compounds, except Fe ₂ O ₃ .	[38]
ZnO, CaO, Fe ₂ O ₃ and MgO	Poplar wood-polypropylene composite	Py-GC/MS	CaO eliminated carboxylic acids and phenols, while slightly increasing cyclopentanones and alkenes.	[110]
Al ₂ O ₃ , CaO, MgO, CuO, Fe ₂ O ₃ , NiO, ZnO, ZrO ₂ , TiO ₂ , HZSM-5 and MCM-41	Cotton stalk	Fixed-bed reactor	Al ₂ O ₃ , CaO and NiO showed the best balance between bio-oil yield and deoxygenation.	[111]

Table 2. Cont.

Catalysts	Biomass	Reactor	Main Results	Ref.
Metallic oxides	Mixed metal oxide of BaMg, BaCa, and CaMg	Bagasse	Py-GC/MS	BaMg-MMO showed a yield maximal of 7.3 wt% and selectivity of 44.4% to 4-VP. [112]
	CaO and CaO/MgO	Wood	Auger reactor pilot plant	Decreased acidity and oxygen content. Increased pH and calorific value [113]
	NbxWyOz, NbxAlYOz, NbxMnyOz, and HZSM-5	Beech wood	Fixed-bed reactor	NbxMnyOz performed similarly to HZSM-5. Reduced O/C fraction from 0.34 to 0.15 and 0.17 with HZSM-5 and NbxMnyOz, respectively. [114]
	CaO, Fe/CaO and Ni/CaO	Jatropha residues	Py-GC/MS	Eliminated carboxylic acids. Decreased N and O-compounds (except ketones, esters and aldehydes). Ni/CaO was the best catalyst for aliphatic HC production [115]
Metallic salts	HCOOK, Ni(HCOO) ₂ , and Zn(HCOO) ₂	Corn straw	Fixed-bed reactor	Increased phenols and ketones. Decreased carboxylic acids and esters. [116]
	Fe(NO ₃) ₃ , Fe ₂ (SO ₄) ₃ , FeCl ₂ , and FeCl ₃	Bamboo	Fixed-bed reactor	FeCl ₂ and FeCl ₃ produced a bio-oil rich in ketones. Fe ₂ (SO ₄) ₃ produced a bio-oil rich in acids. [117]
	Ce, Mn, Fe, Co, Ni, Cu and Zn nitrate salts	Eucalyptus	Fixed-bed reactor	Increased CO ₂ yield and gas phase. Increased anhydrosugars (Zn > Co > Mn > Ni > Ce > Cu > catalyst-free) [118]
	MgCl ₂ and ZnCl ₂	Sweet sorghum bagasse	Py-GC/MS	All catalysts modified the biomass degradation profile and increased solid waste. ZnCl ₂ increased furfural. [119]

HC: hydrocarbons; N-compounds: nitrogen content compounds; O-compounds: oxygen content compounds.

Metal oxides are of great interest because of their acid/base or redox properties. In addition, they are non-toxic, widely available, inexpensive and, in general, improve the quality and stability of bio-oil. They can be divided into basic, acidic and transition metal oxides [13]. Calcium oxide (CaO) and magnesium oxide (MgO) are the main representatives of the class of basic metallic oxides [37,120]. Calcium oxide has strong basic sites, while magnesium oxide has moderate strength basic sites [105]. Calcium oxide has been used in a pure form [108,121], modified with other metals [115,122], as a mixed oxide [112,113] or mixed with zeolites [123] in the pyrolysis of biomass. Other species of Ca²⁺ (Ca(OH)₂ and Ca(COOH)₂) have also been used [109]. In addition, several other oxides have been studied, and their performances have been frequently discussed and compared. Potassium oxide (K₂O) [124] and barium oxide (BaO) [112] are some of the basic metallic oxides that have been investigated.

In general, catalysts with basic characteristics benefit the formation of ketones through ketonization and aldol condensation reactions of carboxylic acids [125]. The elimination of carboxylic acids results in the deacidification and deoxygenation of the bio-oil [37,106,108–110,113,123]. Calcium oxide can promote dehydration, decarbonization, decarboxylation and cracking reactions, and thus, generates a bio-oil with decreased oxygen content, low acidity and, consequently, greater stability and calorific value. Studies have also highlighted its tendency to capture carbon dioxide produced by reactions (e.g., ketonization) and to produce calcium carbonate (CaCO₃). In this case, the carbon dioxide content is reduced, while hydrogen and carbon monoxide are increased. The increase in solid phase yield is expected due to the formation of calcium carbonate [108,126].

Chong et al. [106] compared the performance of calcium oxide, magnesium oxide and zinc oxide in the fast pyrolysis of fiber-derived fruit in a fixed bed reactor. In general, all oxides improved the quality of the bio-oil. Magnesium oxide showed slightly higher efficiency in the decrease of levoglucosan, resulting in the deoxygenation of bio-oil. The reduction was attributed to the decomposition properties of magnesium oxide. Although

magnesium and zinc oxides decreased bio-oil acidity, calcium oxide was the most efficient in deacidifying the bio-oil, through the conversion of carboxylic acids to ketones and the dehydration of carbon dioxide. The increase in water content was observed for all catalysts and assigned to dehydration at high temperatures [106].

Basic metallic oxides impregnated with metals and mixed metallic oxides have been investigated in the pyrolysis of biomass in order to increase the catalytic activity of the simple oxide. Vichaphund et al. [115], for instance, evaluated the performance of calcium impregnated with 5 wt% iron (Fe/CaO) or 5 wt% nickel (Ni/CaO) in the pyrolysis of jatropha residues over different biomass/catalyst ratios (1/1 and 1/5). Impregnation altered the textural characteristics, such as specific surface area, pore volume and pore size, measured by nitrogen adsorption-desorption, in addition to the acidic characteristics of the oxide. The strength and number of basic sites increased, and some acidic sites were created, according to their determination by carbon dioxide temperature-programmed desorption (CO₂-TPD) and ammonia temperature-programmed desorption (NH₃-TPD), respectively. The characterization of the pyrolysis vapors showed that the catalysts decreased nitrogen and oxygen content as a result of denitrogenation and deoxygenation reactions (decarbonization, decarboxylation and cracking), respectively. Carboxylic acids and sugars were completely eliminated through decarboxylation reactions. In particular, the catalysts, Ni/CaO (47.5%), considerably increased the aliphatic hydrocarbon content [115].

In another work, Li et al. [112] investigated a selective catalyst for the production of 4-vinyl-phenol (4-VP) through bagasse pyrolysis. The study showed that by-product formation is inhibited by catalysts with strong basic sites (calcium and magnesium oxides), while 4-VP precursors were not catalyzed. On the other hand, barium oxide, which has low basicity, showed the opposite behavior and low selectivity. Several mixed oxides were proposed to adjust the basicity of the catalyst and increase the selectivity of 4-VP. Among the mixed catalysts, barium-magnesium mixed oxide (BaMg-MMO) led to a maximum yield of 7.3 wt% and showed a selectivity of 44.4%, compared to 5.0 wt% observed in non-catalyzed pyrolysis [112].

Catalysts based on basic and transition metal oxides are the most suitable for the production of phenolic compounds due to their basic characteristics [101]. However, the production of phenols or any other value-added chemical compound depends not only on the catalyst, but also on the pyrolysis conditions (temperature, reactor, residence time) and biomass characteristics [101].

Transition metal oxides also have acid-base characteristics in addition to redox properties. Examples of transition metal oxides are zinc oxide, nickel oxide, zirconia oxide, iron oxide, niobium oxide and ceria oxide, among others [100–102,110]. Although it is not possible to describe a unique behavior for this class, there is a tendency that the higher the acidity/basicity ratio, the more favorable the catalyst will be to catalyze dehydration, depolymerization, C-C or C-O cleavage and ring-opening reactions. This set of reactions contributes to the reduction of anhydrous sugars and the increase of aldehydes, furans and aliphatic hydrocarbons. Higher acidity catalysts have also exhibited a positive effect on aromatics [38,125] and phenolics formation [101]. Oxides based on cerium, chromium, iron, manganese and vanadium have multiple valences, and can be partially reduced to generate oxygen vacancies, which play important roles in polymerization reactions. However, this approach is still under discussion in the literature. On the other hand, nickel, cobalt or copper oxides can be reduced to metallic form and act in cracking reactions. The reduction of species occurs due to the reducing environment of the pyrolysis process, caused by the hydrogen-rich atmosphere [38,111].

Zhang et al. [38] investigated the effect of nine transition metal oxides (CoO, Cr₂O₃, CuO, Fe₂O₃, Mn₂O₃, NiO, TiO₂, V₂O₅ and CeO₂) on the catalytic pyrolysis of poplar wood in a fixed-bed reactor. All catalysts decreased gas and bio-oil yields and promoted the production of alcohols, furans, ketones, acetic acid and phenolics, except iron oxide. Oxides based on cerium, chromium, copper and iron increased the yield of light organic compounds, indicating the promotion of cracking reactions. On the other hand, the oxides

of vanadium, manganese, titanium and cobalt favored condensation reactions, explaining the increase in heavier organics. The nickel-based catalyst increased the yield of heavy and light organics, indicating that both reactions probably occur due to nickel oxide. Metallic nickel, which acts in the cracking reactions, was confirmed by X-ray diffraction [38].

Locatell et al. [114] evaluated mixed niobium oxides with tungsten, aluminum or manganese in ex situ conversion of wood pyrolysis vapors. The results were compared with a reference catalyst (HZSM-5). Mixed oxides with mesopores contributed to better diffusion of larger compounds and better use of available acid sites. The manganese and aluminum-containing catalysts increased the content of hydrogen and carbon oxides in the gas phase, as well as HZSM-5. All catalysts reduced the oxygen content, the manganese-based sample (−39%) being the most similar to HZSM-5 (−46%), although their acidic characteristics were different, the first showing only Lewis acidic sites. It was not possible to establish a correlation between the acidic properties of the catalysts and those of the bio-oil. However, several studies have shown that, under a large amount of steam produced in pyrolysis, the Lewis acidic sites of niobium oxide can be converted into Brønsted acid sites, which may explain the similar performance to HZSM-5 [114].

5.2.3. Metal Salts Catalysts

Regarding metal salts used in biomass pyrolysis, they are classified as alkali or alkaline earth salts (sodium, potassium, magnesium and calcium salts), transition metal salts (copper, iron, magnesium, nickel and zinc salts) and organic acids (ammonium salts) [11]. The effect of these metallic salts on fast pyrolysis of lignocellulosic biomass has shown varied results, which depend not only on the metal, but also on the related anion. Metallic salts are commonly used in the initial phase of pyrolysis, impregnated to the biomass, by placing biomass in contact with an aqueous solution of the metallic salt of a known concentration and for a certain time. Subsequently, the solution is filtered and dried in an oven to remove moisture [11,37].

The studies carried out with bamboo (a low-cost and very popular material) impregnated with iron salts have shown different results, depending on the salt. The different performances of iron nitrate, iron (II) sulfate, ferrous and ferric chloride and iron (III) sulfate were related to the anion and to the valence of iron [117,118]. In general, iron salts affect biomass decomposition in two ways: (i) decreasing biomass crystallinity during impregnation; and (ii) promoting the breakdown of the glycosidic bond, removing water and accelerating char formation during pyrolysis. Iron nitrate increased the gas yield (carbon dioxide and hydrogen). Ferrous and ferric chloride produced a ketones-rich bio-oil (~86%). On the other hand, (iii) iron sulfate greatly increased the content of acidic compounds (11 to 74%), which are undesirable in bio-oil [117]. The decrease in biomass crystallinity can be related to the hydrolysis of cellulose crystals during iron impregnation. Iron salts are able to break hydrogen linkage bonds of cellulose [127], and then weaken the ether bond between carbohydrates and lignin during hydrolysis reactions [128]. The crystallinity of biomass before and after salt impregnation was detected by X-ray diffraction [117].

The effect of anions on catalyst performance has also been observed for metal nitrates [118]. The pyrolysis of eucalyptus over nitrate-based catalysts (mainly manganese, nickel and cerium) also led to an increase in gaseous product yields, mainly carbon dioxide. This indicates that nitrates promoted decarboxylation reactions, which play an important role in bio-oil deoxygenation. In this study, the production of anhydrous sugars was also investigated. Specific compounds of the class of anhydrosugars (1-hydroxy-(1R)-3,6-dioxabicyclo[3.2.1]octan-2-one) were detected during pyrolysis of eucalyptus impregnated with several nitrates, including zinc and cobalt nitrate.

Magnesium chloride and zinc chloride are also able to modify the biomass degradation profile and distribution of pyrolysis products. Both catalysts increased furfural (especially zinc chloride) and char content. In this case, the decrease in the biomass decomposition temperature may have been responsible for inhibiting the pyrolysis of lignin and the

cleavage of the holocellulose rings, favoring the depolymerization of holocellulose to form furfural [119].

It has been found [116] that organic salts increase the yields of phenols and ketones, and decrease the content of highly oxygenated compounds (carboxylic acids and esters). The effect of potassium formate, nickel formate, zinc formate, nickel chloride, potassium chloride and zinc chloride on corn straw pyrolysis, for instance, was investigated by Jiang H. [116]. The formates showed different behaviors due to their physicochemical properties and the catalytic action of the metal cation. The bio-oil yield was increased by nickel formate, followed by zinc formate. At high temperatures, formates were decomposed into hydrogen and other compounds. Hydrogen reacted with organic fragments to form a liquid product. Nickel catalyzes hydrogenation, explaining the high yield of bio-oil. On the other hand, potassium formate promotes secondary reactions of primary compounds due to the strong catalytic activity of potassium, which may also be related to the increase in phenols production. Hydrogen also enhanced the hydrogenation of acidic functional groups that promote the dehydroxylation of acids to form ketones, whereas the reactivity of the metal enhances the cleavage of esters, especially on potassium formate.

5.2.4. Acidic and Basic Carbonaceous Catalysts

The acidic and basic properties of activated carbons are related to the surface functional groups, generated by the interaction of the carbon atoms and heteroatoms, such as oxygen, nitrogen, hydrogen, sulfur and phosphorus. They are mainly formed by the most reactive carbon atoms on the surface, such as the edges of the carbon particles and the delocalized electrons of the structure [129]. The kind and the amount of these groups depend on the precursor material, or on their introduction during the activation process or through special treatments [129,130]. Oxygen is the most important heteroatom, influencing the application of activated carbon, since they affect the electrical and catalytic properties of activated carbons [130].

Ketones, phenols, ethers and lactones (formed from oxygen) groups, as well as amines, nitro and phosphate groups, can determine the acidity or the basicity of activated carbons. Functional groups containing oxygen are the most abundant due to the susceptibility of the carbon surface to react with oxygen in the air [131]. Acid surfaces are characterized by carboxylic, phenolic, lactone, carboxylic anhydride and peroxide groups. The oxygen atoms present in carbonyl groups and ethers are neutral, or can form basic structures. On the other hand, quinones, chromenes and pyrones are responsible for the basic character of activated carbon. The acidic groups are well known, while the basic surfaces of charcoal still remain under investigation [130]. Figure 8 illustrates the functional groups on the coal surface [129]. The presence of acid groups gives activated carbon a more hydrophilic character, in addition to affecting the specific surface area and pore structure [132].

Although several works have addressed the use of activated carbon for pyrolysis of lignocellulosic biomass (Table 1), only a few of them correlated catalyst performance with the surface groups. Ye et al. [73] studied the performance of different catalysts to selectively produce levoglucosenone, by fast pyrolysis of cellulose and biomass (sugar cane bagasse, poplar wood and pine wood). The carbon-based catalysts were prepared from sugar cane bagasse and activated by different methods: chemical activation, using phosphoric acid and zinc chloride, and physical activation, using steam and carbon dioxide. They were compared to a strong acid catalyst (sulfated zirconia). From X-photoelectronic spectroscopy, it has been noted that all catalysts have oxygenated groups, while the carbon activated with phosphoric acids also has C-O-PO₃ and C-PO₃ groups. These groups were related to the highest selectivity of these catalysts in levoglucosenone production.

Some years later, Zhan et al. [75] studied activated carbons enriched in phosphorus-containing functional prepared by one-pot microwave-induced pyrolysis of corn stover. Phosphorous groups, such as -O-P, O=P and -O-P-O-, have been considered the active sites for producing monophenol from cellulose pyrolysis for the first time. The highest yield (44.3 wt%) was obtained with an acid-to-biomass ratio of 0.85.

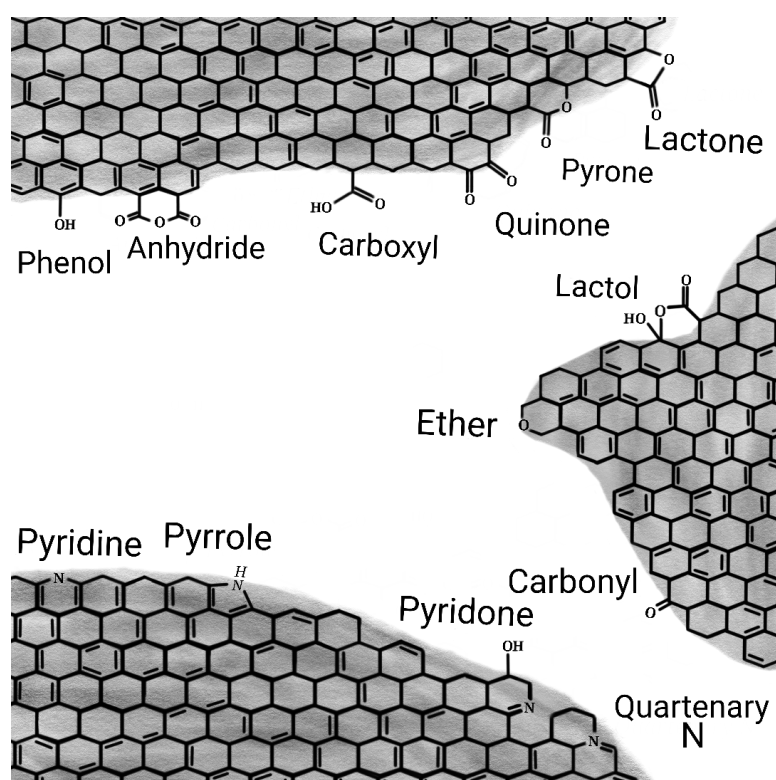


Figure 8. An illustration of functional groups on the carbon surface.

On the other hand, Yang et al. [61] demonstrated the role of oxygenated groups in catalyzing biomass pyrolysis to produce high value products. The catalysts were prepared in bamboo-derived biochar activated at 1073 K, using potassium hydroxide, potassium carbonate, potassium hydrogen carbonate or potassium acetate. During the catalytic pyrolysis, the bio-oil yield decreased, and the gas yield increased, while phenols and aromatics yield significantly increased, and the number of oxygenated species and acetic acid decreased. It has been concluded that activated biochar catalysts act as both catalyst and reactants during the catalytic pyrolysis process.

5.3. Redox Properties of the Catalysts

The redox properties of catalysts for biomass pyrolysis are mostly related to the metal supported on different solids, giving rise to bifunctional catalysts. They play an important role in the process of producing fuels and chemicals, since they usually show a selectivity higher than the acidic or basic catalysts. This is related to the activity of metals in several reactions that occur in pyrolysis, and especially in hydrogenation/dehydrogenation reactions, which occur by a redox mechanism.

5.3.1. Zeolites-Based Catalysts

Several metals, such as noble metals (palladium, ruthenium, platinum) [133,134] and transition metals (cobalt, molybdenum, iron and copper) [96,135,136] can be added to zeolites to obtain bifunctional catalysts. As noted in several works, metal loading can decrease the number of Brønsted acid sites and increase the amount of Lewis acid sites. The specific surface area can also be affected due to metallic species that can block the pores of the zeolites. Table 3 shows some examples of bifunctional catalysts containing different metals at different loadings.

Iron-based catalysts have been used in many studies to obtain upgraded bio-oil. However, iron decreases PAH (especially naphthalene) yields during pyrolysis and enhances BTEX production [54]. This behavior suggests that iron can inhibit the secondary cyclization of monoaromatics to form polyaromatics. This results in a decrease in bio-oil and an

increase in gas production [137]. In agreement with these results, Dai et al. [138] noted that iron on hierarchical HZSM-5 negatively impacts aromatic yields, despite the tendency of producing more monoaromatics and less PAH [138]. Similar results were found by Zhang et al. [137], who reported that the yield of upgraded bio-oil decreased during pyrolysis of rice husks over high iron loading on ZSM-5. They observed non-significant changes in hydrocarbon yield above 4% iron loading in ZSM-5. This finding was related to the decrease in the specific surface area, increasing mass transfer resistance [137].

Copper has also been investigated as zeolite-based catalysts for biomass pyrolysis. Kumar et al. [139], for example, compared the deoxygenating activity of copper and iron over a commercial zeolite catalyst (25% silica-alumina, 0.35% Na₂O) for bio-oil pyrolysis of pine wood. They noted that the copper-based catalyst produced 5.05% phenols and 1.16% ketones, whereas the nickel-based zeolite generated 2.24% phenols and 1.02% ketones; no aldehyde was detected in any bio-oil sample. Despite this, the addition of metal promoted greater production of aromatics than the non-catalytic pyrolysis, especially at high catalyst/biomass ratios. This was related to the higher amount of available active sites, resulting in more deoxygenation of bio-oil and in the production of hydrocarbons [104].

A combination of the two metals has also been used in zeolite catalysts for biomass pyrolysis, generating bimetallic catalysts. This takes advantage of the possible synergistic effect that can promote different reactions, improving the final bio-oil [140]. Zheng et al. [141], for example, evaluated the activity and selectivity of nickel and copper supported on HZSM-5, during the pine wood conversion for producing bio-aromatic and bio-phenols. The bimetallic catalysts showed higher deoxygenation efficiency than the monometallic ones. Higher nickel loads promoted decarbonylation, decarboxylation and aromatization reactions, while higher copper loading increased the yields of olefins and phenols due to the dehydration and demethylation reactions [141]. Molybdenum combined with cobalt, iron or nickel supported on hierarchical HZSM-5 have also been investigated [142]. The NiMo/ZSM-5 catalyst exhibited less coke and converted more high-order graphite carbon to low-order carbon than the other catalysts. In addition, it showed the highest MAH production and the minimum selectivity of oxygenates.

Table 3. Several metal loadings zeolites used in catalytic fast pyrolysis.

Metal Loading	Zeolite Framework	Feedstock	Operational Conditions	Ref.
Ga	HZSM-5	Cotton-stalk	T: 723–1123 K t: 20 s hr: 20 K/ms	[143]
Fe, La, Cu, Mg, Al and Ce	ZSM-5	Cellulose	T: 873 K p(N ₂): 300 mL/min t: 30 min	[144]
Zn	HZSM-5	Milled wood Lignin	T: 923 K t: 20 s	[145]
none	HY, USY		hr: 20 K/ms	
none	ZSM-5/H-Beta	Wood polymer composites	T: 773–873 K t: 20 K/min	[53]
none	Y-zeolite	Coal	T: 973 °C t: 10 K/ms hr: 15 s	[146]
none	HY-zeolite	Baiyinhua lignite	T: 873 K p(N ₂): 300 mL/min t: 30 min	[147]
none	HY-zeolite	Waste Engine Oil	T: 773 K p(N ₂): 80 mL/min	[148]
Ni	ZSM-5	Lignin	T: 723 K p(N ₂): 97 cm ³ /min t: <5 s	[149]
Fe	ZSM-5	Wood sawdust	T: 553 K p(N ₂): 30 mL/min hr: 10 K/min	[150]
Sr, Ni, Cu, Ag and Fe	Y-zeolite	Waste cooking oil	T: 823–1023 K t: 30 s hr: 10 K/min	[151]

T: temperature; t: residence time; hr: heating rate.

5.3.2. Oxide-Based Catalysts

The addition of metals to oxides aims to promote the catalytic activity of the simple oxide through the combination of the acidic or basic sites of the support and the metallic sites of the impregnated metal. Although it is not possible to attribute a single behavior to these bifunctional catalysts, studies have shown that metal impregnation (noble metals, nickel, iron and cobalt) alters the acidic and textural characteristics of the support, leading to a reduction in the content of oxygenated compounds and nitrogenous [115,120,152].

Zhang et al. [153] impregnated iron on calcium oxide, obtaining a bifunctional catalyst that was used in sawdust pyrolysis. Iron prevented catalyst deactivation and the bifunctional catalyst converted heavy phenols into light phenols, eliminating acidic compounds and decreasing the content of aldehydes and ketones. In contrast, furans, light and aromatic hydrocarbons were increased. The better performance of the bifunctional catalyst was related to the synergistic action between calcium oxide and iron, forming the active $\text{Ca}_2\text{Fe}_2\text{O}_5$. A similar effect was found by Sun et al. [122].

Kantarelis, Yang and Blasiak [154] investigated the effects of nickel and vanadium supported on silica on the composition of pyrolysis vapors from a mixture of pine and spruce. Both catalysts were active in vapor deoxygenation and phenol production. The nickel catalyst was selective to aromatics, while the vanadium catalyst decreased acids and ketones. The in situ reduction of nickel oxide during pyrolysis reactions was supposed to potentiate H transfer reactions during the process.

6. Catalyst to Biomass Ratio

Catalyst loading is also an important variable to be considered in biomass pyrolysis as it significantly affects the yield and distribution of the products. This dependence is related to catalyst activity in deoxygenation reactions, releasing oxygen as water and carbon monoxide and dioxide. It has been found [16] that dehydration is a dominant pathway when the catalyst-to-biomass ratio is very low, and that decarbonylation increases with increasing catalyst amounts. The optimal catalyst/biomass ratio was found to be between 0.3 and 0.7 [155]. Higher catalyst loading can lead to excessive cracking of pyrolytic vapors and lower bio-oil yields, in addition to fast catalyst deactivation by coke [156]. Excessive deoxygenation under higher catalyst loading also increases aromatic fractions in pyrolysis liquids [157].

By studying the pyrolysis of paddy husk over a ZSM-5 catalyst, Naqvi et al. [158] found that bio-oil and bio-char yields decreased, and gas yields increased with an increasing in catalyst-to-biomass ratios. The lowest ratio (0.5) led to the maximum bio-oil yield (35.5%). The bio-oil yields decreased from 42% to 30% by increasing the catalyst from 5% to 20%. In addition, Zhou et al. [159] found that bio-oil yields decreased by 6%, but the yields of small molecule compounds in bio-oils increased with an increasing zinc oxide catalyst (5–20%). Furthermore, at higher amounts of catalyst, deoxygenation of unwanted species increased in gas yields from 21.38% to 28.74% (wt.), while biochar yields did not significantly change. Several operational challenges related to tar formation in pipes resulted from the use of high amounts of the basic catalyst (calcium oxide), causing a decrease in bio-oil yields and favoring secondary reactions to volatiles and tar, as reported by Veses et al. [113]. In another work, using sepiolite, it has been found that excess amounts of the catalyst were not appropriate for obtaining higher bio-oil yields. Decreasing the amounts of sepiolite, the bio-oil and gas yields were increased with a sharp drop in bio-char [160].

In general, the higher the loading of acidic zeolite, the lower the bio-oil production. Increasing the catalyst-to-biomass ratio from 1:2 to 1:1, for instance, bio-oil yields decreased from 50.41% to 29.37% *w/w* [161]. On the other hand, a higher catalyst-to-biomass ratio produces more hydrocarbons, while the relative amounts of oxygenates (ketones, aldehydes and carboxylic compounds) significantly decreased. Therefore, high-quality bio-oil (rich in hydrocarbons and poor in oxygenates) can be obtained over zeolites, such as ZSM-5; a fact that is also related to its tridimensional intersecting pore structure. The increase in catalyst-to-biomass ratio and of a unit mass of zeolite facilitates the diffusion of large

molecules into internal channels, where they produce smaller hydrocarbons and coke deposition [157].

7. Co-Pyrolysis of Biomass and Hydrogen Donors

One of the most important differences between biomass and oil feedstocks is the high number of oxygenated compounds in the former. This difference in composition prevents the use of most of the mature technologies developed for petroleum refining in new biorefineries. This has motivated researchers to look for efficient methods for the removal of oxygen, such as water, carbon monoxide and carbon dioxide, or other compounds, such as alcohols, aldehydes and acids. However, this consumes carbon and hydrogen during pyrolysis, decreasing the efficiency of the process. To overcome this problem, the technology of co-pyrolysis was proposed, in which pyrolysis of biomass occurs in the presence of some hydrogen donors, such as plastics, ethanol and methanol, to prepare liquid fuels and high value-added chemicals [13]. Among them, plastic residues emerge as the most economical and environmentally friendly option, because of their large consumption around the world. It is estimated that the worldwide generation of plastic-based waste is around 1.3 billion tons per year, and a value of 2.2 billion tons is expected over the next few years [162].

Several types of catalysts have been evaluated in the co-pyrolysis of biomass and plastics, such as metal oxides, alumina, spent FCC (Fluid Catalytic Cracking) catalysts and zeolites. Spent FCC and larger-pore zeolites are suitable for obtaining liquid hydrocarbons; zeolites being especially appropriate due to large specific surface areas, thermal stability and high acidity. In addition, the cooperative action of these properties can be adjusted to promote bio-oil formation and/or to inhibit solids production [13,162].

An alternative by which to enhance selectivity towards aromatic hydrocarbons, during biomass pyrolysis, is the addition of plastics, such as low-density polyethylene (LDPE), generating the so-called co-pyrolysis. In this process, hydrogen is supplied to the reaction as the hydrogen-to-carbon ratio of LDPE is higher than that of biomass. Furthermore, the use of both species tends to inhibit catalyst deactivation, as well as to reduce solid residue formation. For example, Zheng et al. [163] studied the co-pyrolysis of LDPE and pine sawdust (cellulose), and found an improvement in BTEX yield and selectivity to naphthalene and naphthalene-derived species, while lowering the compounds bigger than C10 aromatics. Yang et al. [164] studied LDPE co-pyrolysis with cedarwood, sunflower stalk and *Fallopia japonica* stem at a maximum temperature of 600 °C. The pyrolysis of only cedarwood yielded 38.3% of bio-oil, 14.7% of gas, 25.74% of water and 20.73% of char. When LDPE was added to biomass, oil yields jumped up to 64.08%, with 7.98% of the yield being the gas phase, 15.94% being water, 9.32% being residual solids and 2.69% being wax.

Co-pyrolysis of biomass and high-density polyethylene (HDPE) can improve selectivity when compared to HDPE pyrolysis. Rahman et al. [165], for instance, performed co-pyrolysis *ex situ* of HDPE and pine sawdust at different ratios (0:100, 25:75 and 50:50 and at 723, 773 and 823 K) over ZSM-5. As expected, low ratios of biomass-to-plastic yielded the smallest percentage of bio-oil, while raising the temperature made HDPE decomposition easier. At 823 K, a decrease in yield was noted, probably due to the further cracking of species into even lighter species. At high biomass-to-plastic ratios, the inverse trend was observed. At 25-to-75 or 50-to-50 ratios, there was no noticeable temperature effect on the liquid phase yield. However, by raising the biomass fraction, the liquid yield was raised at low temperatures, as expected, since low temperatures favor biomass pyrolysis. At higher temperatures, the condensable species cracked even more into non-condensable ones. The solid residue presented both molten plastic and pine fibers, probably due to the effect of molten plastic, which hindered the pyrolysis of biomass fibers. This effect also explains the less oil yield when more char was generated. The highest bio-oil yield (22.5%) was obtained at 25-to-75 ratio and 500 °C, with 7.3% of solids and 69.7% of gasses. Varying the pine-to-HDPE ratio from 100 to 0, 75 to 25, 50 to 50, 25 to 75 and 0 to 100, the selectivity for

gasoline-ranged hydrocarbons was 68.9%, 94.5%, 100%, 98.7% and 100%, respectively, at 523 K. This effect can be explained by the gradual increase in the hydrogen-to-carbon ratio.

In another work, Hassan, Hameed and Lim, [166] studied the co-pyrolysis of HDPE and sugarcane bagasse in the range of 673–973 K, using biomass-to-plastic ratios from 0% to 100%. The highest bio-oil yield was noted at 873 K, at a 3-to-2 ratio, the formation of oxygenated compounds was inhibited, and the production of aromatics, hydrocarbons and alcohol was promoted.

Co-pyrolysis of polyethylene terephthalate (PET) and biomass can reduce the generation of aromatic polycyclic species, operating under moderate temperatures; however, under higher temperatures, such species formation tends to increase. Izzatie et al. [167] carried out rice straw and PET co-pyrolysis at a 1-to-1 ratio in a fixed-bed reactor, under 723, 773, 823 and 873 K. They obtained 36% of bio-oil, 44.67% of gasses and 19.33% of solid residue. Çepeliogullar and Pütün, [168] co-pyrolyzed hazelnut shell and PET, at a 1-to-1 ratio, at 773 K. Compared to pyrolysis of biomass alone, the bio-oil and gas fractions presented higher yields (10.67% and 6.40%, respectively), while water and solid production decreased by 13.56% and 4.67%, respectively. The bio-oil obtained from biomass-only contained 79.85% of phenolic species, while the bio-oil from co-pyrolysis was composed of 4.64% phenolic species, 22.42% benzene-derived species and 59.83% acids and esters.

Izzatie et al. [167] co-pyrolyzed rice straw and polypropylene (PP) at a 1-to-1 ratio under similar operating conditions using rice straw and PET. The highest yield of the oil fraction was 69% at 823 K, along with 20.5% gasses and 10.5% solid residue. The bio-oil was also composed of furfural, 2-methyl naphthalene, tetrahydrofuran, toluene and acetaldehyde.

Abnisa et al. [169] performed co-pyrolysis of palm shells and polystyrene (PS) in a fixed-bed reactor at 400 °C and a 4:6 biomass-to-plastic ratio, obtaining 65% bio-oil yield, 20% gasses and 15% char. Stancin et al. [170] co-pyrolyzed sawdust and solid waste-recovered PS in fixed-bed reactors, operating at 873 K under various biomass-to-plastic ratios. The highest yield of oils was of 84% at a 3-to-1 ratio; the lowest being 62% at a 1:3 ratio.

One of the advantages of co-pyrolysis of polyvinyl chloride (PVC) is less emission of polyaromatic hydrocarbons, such as acenaphthylene, naphthalene, acenaphthene and others, as well as less hydrochloric acid generation. While pyrolyzing rice husk and PVC over magnesium oxide and magnesium carbonate, a slight decrease in acid content and increased hydrocarbon generation over 35% was observed [171]. Çepeliogullar and Pütün [168] performed co-pyrolysis of hazelnut shell and PVC in a fixed-bed reactor at 773 K and at a 1-to-1 ratio. The pyrolysis of only hazelnut shells generated 18.22% bio-oil (containing 79.85% of phenolics), 18.17% water, 33.51% of non-condensable gasses and 30.1% of solid residue. Meanwhile, the co-pyrolysis produced 15.26% of oil (no phenolic species, but 51.3% of naphthenic derivatives), 15.34% of water, 43.62% of gasses and 25.78% of residues. In another work [172], a previous PVC dichlorination step decreased 75 wt% of chlorine in the liquid fraction, but also decreased catalyst activity. It was not clear if the activity loss was related to physical mechanisms (such as molten plastic blocking the catalyst pores) or to chemical mechanisms (such as conventional catalyst poisoning).

8. Guidelines for Selecting Catalysts for Pyrolysis of Lignocellulosic Biomass

Catalytic pyrolysis offers new opportunities to produce high quality fuels and chemicals by an economical, eco-friendly and simple route using lignocellulosic biomass, a cheap and widespread feedstock. The properties and the availability of different kinds of catalysts make possible the accurate design of a solid focusing mainly on the specific surface area and porosity, the strength and distribution of acidic and basic sites, as well as redox properties, which are responsible for catalytic activity and selectivity towards the desired products. Because of the complexity of biomass, pyrolysis involves a reaction network with numerous different pathways, each one affected by the catalyst according to its own kinetics. The kind of biomass and the process variables, such as temperature,

heating rate, biomass-to-catalyst ratio and use of hydrogen donors, among others, also affect the reactions. This dependence requires a specific catalyst and the optimization of the process variables for each biomass. This makes catalyst design strongly dependent on experimental research. In spite of this, the relationships between the catalyst properties and the pyrolysis products, discussed in this review, can provide a guideline for accelerating the experimental studies to achieve the target products, as shown below.

1. The acidic sites facilitate the breaking of C-C and C-O bonds, and then are able to catalyze the majority of reactions that occur during the pyrolysis of lignocellulosic biomass, such as cracking, aromatization, dehydration, decarboxylation, decarbonylation, oligomerization, polymerization/depolymerization, ketylation and H-transfer reactions.
2. The metallic sites act cooperatively with the acidic sites through a bifunctional mechanism, and also promote hydrogenation/dehydrogenation reactions.
3. Acidic zeolites and hierarchical zeolites are the most studied catalysts for lignocellulosic biomass pyrolysis because of intrinsic acidity and large pores. In addition, the pores can be tailored to favor the formation of the desired products by shape selectivity. Due to these properties, they are the best option by which to obtain monoaromatics, such as the high-value benzene, toluene and xylenes (BTX), without polyaromatics and coke formation. However, large pores can also allow the production of undesirable polyaromatics, which, in turn, can be avoided by the metal. Therefore, the pores have to be modulated. The use of a metal is usually beneficial in such cases.
4. Catalysts based on acidic metal oxides usually lead to the production of aromatics, anhydrosugars and furans, in addition to gasses and solids, during pyrolysis of lignocellulosic biomass; however, the kind and distribution of products depend on the metal oxide.
5. Activated carbons are normally used to catalyze the production of levoglucosenone and phenols. The activity and selectivity of such catalysts are modulated by functional groups on the surface.
6. Alkali and alkaline earth metal oxides selectively catalyze the formation of phenolic compounds, ketones and furans, but also produce high-quality bio-oil. On the other hand, transition metal oxides are the most suitable to produce phenolic compounds because of their basic properties. The balance between acidic and basic sites affects the distribution of products obtained thanks to the formation of other compounds, such as alcohols, furans, ketones and phenolics.
7. Basic zeolites (modified with a basic component) are also active and selective in biomass pyrolysis producing high quality bio-oil, due to a decrease in oxygenates and acidic compounds, and a small amount of coke. They are usually more active than acidic zeolite in deoxygenation.
8. The catalyst-to-biomass ratio is a critical process variable for catalyst performance during biomass pyrolysis, the optimal ratio being found between 0.3 and 0.7. However, this range may change according to the catalyst, variable processes and biomass.
9. The efficiency of pyrolysis of lignocellulosic biomass can be largely improved by adding hydrogen donors to the process (co-pyrolysis), such as plastics, ethanol and methanol. Several plastics have been studied, including low- (LDPE) and high (HDPE)-density polyethylene, polyethylene terephthalate (PET), polypropylene (PP), polystyrene (PS), polyvinyl chloride (PVC) and plastic residues. The latter is particularly attractive for environmental reasons.
10. Obtaining target products from biomass pyrolysis requires the careful planning of catalyst properties combined with the process variables according to the biomass to be used. Co-pyrolysis of plastic residues is attractive as an economic and eco-friendly route, providing clean fuels and chemicals, as well as decreasing plastic waste around the world.

Author Contributions: Conceptualization, writing—original draft preparation, writing—review and editing: F.M.M., M.d.S.C., G.S. and A.M.d.A. Conceptualization, writing—original draft preparation, writing—review and editing, supervision: M.d.C.R. All authors have read and agreed to the published version of the manuscript.

Funding: This research was funded by the Brazilian National Oil, Gas and Biofuel Agency (ANP) through the Human Resources Program and by Coordenação de Aperfeiçoamento de Pessoal de Nível Superior—Brasil (CAPES), grant number 001.

Institutional Review Board Statement: Not applicable.

Informed Consent Statement: Not applicable.

Data Availability Statement: Not applicable.

Conflicts of Interest: The authors declare no conflict of interest.

Abbreviation

AH	aromatic hydrocarbon
Al-MCM-41	Mobil Composition of Matter-forty-one impregnated with aluminum
Al-Fe-MCM-41	Mobil Composition of Matter-forty-one impregnated with aluminum and iron
ASU-7	Arizona State University (seven) ($[(DMA)_2(H_2O)_2][Ge_{20}O_{40}]$ where DMA = dimethylamine)
ASV	Arizona Seven, (group, $[(DMA)_2(H_2O)_2][Ge_{20}O_{40}]$ where DMA = dimethylamine)
AZ	Hierarchical HZSM-5 obtained by conventional desilication
AZM	micro-mesoporous composite catalyst produced by alkali treatment
BEA	Zeolite Beta polymorph A, (group $Na_7[Al_7Si_{57}O_{128}]$)
BTEX	benzene, toluene, ethylbenzene, and xylenes
BTX	benzene, toluene, and xylenes
CO ₂ -TPD	carbon dioxide temperature-programmed desorption
Cu-MCM-41	Mobil Composition of Matter-forty-one impregnated with copper
FCC	Fluid Catalytic Cracking
Fe-MCM-41	Mobil Composition of Matter-forty-one impregnated with iron
HC	hydrocarbons
HDO	hydrodeoxygenation
HDPE	high density polyethylene
hr	heating rate
ISV	Instituto de Tecnologia Quimica Valencia (seven) (group, $Si_{64}O_{128}$)
ITQ-7	Instituto de Tecnologia Quimica Valencia (seven) ($Si_{64}O_{128}$)
ITE	Instituto de Tecnologia Quimica Valencia (three) (group, $Si_{64}O_{128}$)
ITQ-3	Instituto de Tecnologia Quimica Valencia (three) ($Si_{64}O_{128}$)
LDPE	low density polyethylene
LTA	Linde Type A, (group, $[Na_{12}(H_2O)_{278}]_8[Al_{12}Si_{12}O_{48}]_8$)
MAH	monoaromatic hydrocarbon
MCM-41	Mobil Composition of Matter-forty-one, SiO_2
MDF	medium density fiber
MEL	Mobil—eleven (group, $Na_x(H_2O)_{16}[Al_xSi_{96-x}O_{192}]$ ($x < 16$))
MFI	Mobil—five (group, $Na_x(H_2O)_{16}[Al_xSi_{96-x}O_{192}]$ ($x < 27$))
MOR	Mordenite, (group, $Na_8(H_2O)_{24}[Al_8Si_{40}O_{96}]$)
MWW	Mobil Twenty-two (group, $[H^{+2.4}Na^{+3.1}Al_{0.4}B_{5.1}Si_{66.5}O_{144}]$)
MCM-22	Mobil Composition of Matter (Twenty-two) ($[H^{+2.4}Na^{+3.1}Al_{0.4}B_{5.1}Si_{66.5}O_{144}]$)
N-compounds	nitrogen content compounds
NH ₃ -TPD	ammonia temperature-programmed desorption
NiMo/AZM	Micro-mesoporous hierarchical zeolite impregnated with nickel and molybdenum
Ni/beta zeolite	Beta zeolite impregnated with nickel
Ni/ZSM-5	Zeolite Socony Mobil—five impregnated with nickel
O-compounds	oxygen content compounds
OFF=ZSM-34	Offretite, (group, $(Ca, Mg)_{1.5}K(H_2O)_{14}[Al_4Si_{14}O_{36}]$)
PAH	polyaromatic hydrocarbon

PET	polyethylene terephthalate
PP	polypropylene
PS	polystyrene
PVC	polyvinyl chloride
Py-GC/MS	Pyrolysis-gas chromatography-mass spectrometry
SBA-15	Santa Barbara Amorphous-fifteen, SiO ₂
SSY	Standard Sixty (group, [B _{0.75} Si _{26.25} O ₅₄])
SSZ-60	Standard Oil Synthetic Zeolite—sixty ([B _{0.75} Si _{26.25} O ₅₄])
t	residence time
T	temperature
ZSM-11MEL	Zeolite Socony Mobil—eleven, Na _x (H ₂ O) ₁₆ [Al _x Si _{96-x} O ₁₉₂] (x < 16)
ZSM-34=OFF	Zeolite Socony Mobil—thirty-four, (Ca, Mg) _{1.5} K(H ₂ O) ₁₄ [Al ₄ Si ₁₄ O ₃₆]
ZSM-5=MFI	Zeolite Socony Mobil—five, Na _x (H ₂ O) ₁₆ [Al _x Si _{96-x} O ₁₉₂] (x < 27)
Z@M	core-shell (ZSM-5 and MCM-41) hierarchical zeolite

References

1. Ayhan, D. *Biorefineries—For Biomass Upgrading Facilities*; Springer: London, UK, 2010. [CrossRef]
2. Zhang, L.; Bao, Z. Catalytic Pyrolysis of Biomass and Polymer Wastes. *Catalysts* **2018**, *8*, 659. [CrossRef]
3. Basu, P. *Biomass Gasification and Pyrolysis: Practical Design and Theory*; Elsevier: Burlington, UK, 2010; pp. 1–365. [CrossRef]
4. Yan, K.; Li, H. State of the Art and Perspectives in Catalytic Conversion Mechanism of Biomass to Bio-aromatics. *Energy Fuels* **2021**, *35*, 45–62. [CrossRef]
5. Serio, M.A.; Kroo, E.; Wójtowicz, M.A. Biomass pyrolysis for distributed energy generation. *Am. Chem. Soc. Fuel Chem.* **2003**, *48*, 584–589.
6. Rangel, M.C.; Carvalho, M.d.S.; Mayer, F.M.; Saboia, G.; de Andrade, A.M.; de Oliveira, A.P.S.; dos Santos, P.L. Improving Fast Pyrolysis by Tailoring High-Quality Products Using Catalysts. In *Advances in Chemistry Research*, 1st ed.; Taylor, J., Ed.; Nova Publishers: New York, NY, USA, 2022; Volume 75, pp. 119–169.
7. Chio, C.; Sain, M.; Qin, W. Lignin utilization: A review of lignin depolymerization from various aspects. *Renew. Sustain. Energy Rev.* **2019**, *107*, 232–249. [CrossRef]
8. Ong, H.C.; Chen, W.; Farooq, A.; Gan, Y.Y.; Lee, K.T.; Ashokkumar, V. Catalytic thermochemical conversion of biomass for biofuel production: A comprehensive review. *Renew. Sustain. Energy Rev.* **2019**, *113*, 109266. [CrossRef]
9. Lyu, G.; Wu, S.; Zhang, H. Estimation and comparison of bio-oil components from different pyrolysis conditions. *Front. Energy Res.* **2015**, *3*, 28. [CrossRef]
10. Kim, J.-S.; Choi, G.-G. Pyrolysis of lignocellulosic biomass for biochemical production. In *Waste Biorefinery: Potential and Perspectives*; Elsevier: Amsterdam, The Netherlands, 2018; pp. 323–348. [CrossRef]
11. Guilhaume, N.; Schuurman, Y.; Geantet, G. The role of catalysis in the valorization of woody biomass fast pyrolysis liquids: Overview and contribution of IRCELYON. *Catal. Today* **2021**, *373*, 5–23. [CrossRef]
12. Zhang, M.; Hu, Y.; Wang, H.; Li, H.; Han, X.; Zeng, Y.; Xu, C.C. A review of bio-oil upgrading by catalytic hydrotreatment: Advances, challenges and prospects. *Mol. Catal.* **2021**, *504*, 111438. [CrossRef]
13. Qiu, B.; Tao, X.; Wang, J.; Liu, Y.; Li, S.; Chu, H. Research progress in the preparation of high-quality liquid fuels and chemicals by catalytic pyrolysis of biomass: A review. *Energy Convers. Manag.* **2022**, *261*, 115647. [CrossRef]
14. Morgan, H.M.; Bu, Q.; Liang, J.; Liu, Y.; Mao, H.; Shi, A.; Lei, H.; Ruan, R. A review of catalytic microwave pyrolysis of lignocellulosic biomass for value-added fuel and chemicals. *Bioresour. Technol.* **2017**, *230*, 112–121. [CrossRef]
15. Carlson, T.R.; Tompsett, G.A.; Conner, W.C.; Huber, G.W. Aromatic production from catalytic fast pyrolysis of biomass-derived feedstocks. *Top. Catal.* **2009**, *52*, 241–252. [CrossRef]
16. Wang, Y.; Akbarzadeh, A.; Chong, L.; Du, J.; Tahir, N.; Awasthi, M.K. Catalytic pyrolysis of lignocellulosic biomass for bio-oil production: A review. *Chemosphere* **2022**, *297*, 134181. [CrossRef] [PubMed]
17. Sahoo, A.; Kumar, S.; Kumar, J.; Bhaskar, T. A detailed assessment of pyrolysis kinetics of invasive lignocellulosic biomasses (*Prosopis juliflora* and *Lantana camara*) by thermogravimetric analysis. *Bioresour. Technol.* **2021**, *312*, 124060. [CrossRef] [PubMed]
18. Duan, Y.; Mehariya, S.; Kumar, A.; Singh, E.; Yang, J.; Kumar, S.; Li, H.; Awasthi, M.K. Apple orchard waste recycling and valorization of valuable product—A review. *Bioengineered* **2021**, *12*, 476–495. [CrossRef]
19. Ansari, K.B.; Arora, J.S.; Chew, J.W.; Dauenhauer, P.J.; Mushrif, S.H. Fast Pyrolysis of Cellulose, Hemicellulose, and Lignin: Effect of Operating Temperature on Bio-oil Yield and Composition and Insights into the Intrinsic Pyrolysis Chemistry. *Ind. Eng. Chem. Res.* **2019**, *58*, 15838–15852. [CrossRef]
20. Jae, J.; Coolman, R.; Mountziaris, T.; Huber, G.W. Catalytic pyrolysis of lignocellulosic biomass in a process development unit with continual catalyst addition and removal. *Chem. Eng. Sci.* **2014**, *108*, 33–46. [CrossRef]
21. Wang, J.; Zhong, Z.; Ding, K.; Deng, A.; Hao, N.; Meng, X.; Ben, H.; Ruan, R.; Ragauskas, A.J. Catalytic fast pyrolysis of bamboo sawdust via a two-step bench scale bubbling fluidized bed/fixed bed reactor: Study on synergistic effect of alkali metals oxides and HZSM-5. *Energy Convers. Manag.* **2018**, *176*, 287–298. [CrossRef]

22. Leng, L.; Yang, L.; Chen, J.; Leng, S.; Li, H.; Li, H.; Yuan, X.; Zhou, W.; Huang, H. A review on pyrolysis of protein-rich biomass: Nitrogen transformation. *Bioresour. Technol.* **2020**, *315*, 123801. [[CrossRef](#)]
23. Rjeily, M.A.; Gennequin, C.; Pron, H.; Abi-Aad, E.; Randrianalisoa, J.H. Pyrolysis-catalytic upgrading of bio-oil and pyrolysis-catalytic steam reforming of biogas: A review. *Environ. Chem. Lett.* **2021**, *19*, 2825–2872. [[CrossRef](#)]
24. Duan, Y.; Pandey, A.; Zhang, Z.; Awasthi, M.K.; Bhatia, S.K.; Taherzadeh, M.J. Organic solid waste biorefinery: Sustainable strategy for emerging circular bioeconomy in China. *Ind. Crops Prod.* **2020**, *153*, 112568. [[CrossRef](#)]
25. Singh, E.; Kumar, A.; Mishra, R.; You, S.; Singh, L.; Kumar, S.; Kumar, R. Pyrolysis of waste biomass and plastics for production of biochar and its use for removal of heavy metals from aqueous solution. *Bioresour. Technol.* **2021**, *320*, 124278. [[CrossRef](#)] [[PubMed](#)]
26. Jiang, L.; Wang, Y.; Dai, L.; Yu, Z.; Yang, Q.; Yang, S.; Jiang, D.; Ma, Z.; Wu, Q.; Zhang, B.; et al. Co-pyrolysis of biomass and soapstock in a downdraft reactor using a novel ZSM-5/SiC composite catalyst. *Bioresour. Technol.* **2019**, *279*, 202–208. [[CrossRef](#)]
27. Tan, Y.L.; Abdullah, A.Z.; Hameed, B.H. Product distribution of the thermal and catalytic fast pyrolysis of karanja (*Pongamia pinnata*) fruit hulls over a reusable silica-alumina catalyst. *Fuel* **2019**, *245*, 89–95. [[CrossRef](#)]
28. Yung, M.M.; Starace, A.K.; Griffin, M.B.; Wells, J.D.; Patalano, R.E.; Smith, K.R.; Schaidle, J.A. Restoring ZSM-5 performance for catalytic fast pyrolysis of biomass: Effect of regeneration temperature. *Catal. Today* **2019**, *323*, 76–85. [[CrossRef](#)]
29. Jerzak, W.; Gao, N.; Kalembe-Rec, I.; Magdziarz, A. Catalytic intermediate pyrolysis of post-extraction rapeseed meal by reusing ZSM-5 and Zeolite Y catalyst. *Catal. Today* **2022**, *404*, 63–77. [[CrossRef](#)]
30. Panahi, H.K.S.; Tabatabaei, M.; Aghbashlo, M.; Dehghani, M.; Rehan, M.; Nizami, A.-S. Recent updates on the production and upgrading of bio-crude oil from microalgae. *Bioresour. Technol. Rep.* **2019**, *7*, 100216. [[CrossRef](#)]
31. Carlson, T.R.; Vispute, T.P.; Huber, G.W. Green gasoline by catalytic fast pyrolysis of solid biomass derived compounds. *Chemsuschem* **2008**, *1*, 397–400. [[CrossRef](#)]
32. Banks, S.W.; Bridgwater, A.V. Catalytic fast pyrolysis for improved liquid quality. In *Handbook of Biofuels Production*, 2nd ed.; Luque, R., Lin, C.S.K., Eds.; Woodhead Publishing: New York, NY, USA, 2016; pp. 391–429.
33. French, R.; Czernik, S. Catalytic pyrolysis of biomass for biofuels production. *Fuel Process. Technol.* **2010**, *91*, 25–32. [[CrossRef](#)]
34. Diebold, J.P. *A Review of the Chemical and Physical Mechanisms of the Storage Stability of Fast Pyrolysis Bio-Oils*; National Renewable Energy Laboratory: Golden, CO, USA, 1999. [[CrossRef](#)]
35. Carvalho, M.; Oliveira, A.P.; Mayer, F.; Virgens, C.; Rangel, M.D.C. Thermokinetic and thermodynamic parameters for catalytic pyrolysis of medium density fiber over Ni/beta zeolite. *Catal. Res.* **2022**, *2*, 1–20. [[CrossRef](#)]
36. Mayer, F.M.; de Oliveira, A.P.S.; Junior, D.L.d.O.; Agustini, B.C.; da Silva, G.A.; Tanabe, E.H.; Ruiz, D.; Rangel, M.D.C.; Zini, C.A. Influence of Nickel Modified Beta Zeolite in the Production of BTEX During Analytical Pyrolysis of Medium-Density Fiberboard (MDF). *Waste Biomass Valorization* **2022**, *13*, 1717–1729. [[CrossRef](#)]
37. Wang, W.; Lemaire, R.; Bensakhria, A.; Luart, D. Review on the catalytic effects of alkali and alkaline earth metals (AAEMs) including sodium, potassium, calcium and magnesium on the pyrolysis of lignocellulosic biomass and on the co-pyrolysis of coal with biomass. *J. Anal. Appl. Pyrolysis* **2022**, *163*, 105479. [[CrossRef](#)]
38. Zhang, C.; Zhang, L.; Li, Q.; Wang, Y.; Liu, Q.; Wei, T.; Dong, D.; Salavati, S.; Gholizadeh, M.; Hu, X. Catalytic pyrolysis of poplar wood over transition metal oxides: Correlation of catalytic behaviors with physicochemical properties of the oxides. *Biomass Bioenergy* **2019**, *124*, 125–141. [[CrossRef](#)]
39. Dickerson, T.; Soria, J. Catalytic fast pyrolysis: A review. *Energy* **2013**, *6*, 514–538. [[CrossRef](#)]
40. Silva, C.L.S.; Marchetti, S.G.; Júnior, A.D.C.F.; Silva, T.D.F.; Assaf, J.M.; Rangel, M.D.C. Effect of gadolinium on the catalytic properties of iron oxides for WGS. *Catal. Today* **2013**, *213*, 127–134. [[CrossRef](#)]
41. Carvalho, L.S.; Martins, A.R.; Reyes, P.; Oportus, M.; Albonoz, A.; Vicentini, V.; Rangel, M.D.C. Preparation and characterization of Ru/MgO-Al₂O₃ catalysts for methane steam reforming. *Catal. Today* **2009**, *142*, 52–60. [[CrossRef](#)]
42. Querino, P.; Bispo, J.R.C.; Rangel, M.C. The effect of cerium on the properties of Pt/ZrO₂ catalysts in the WGS. *Catal. Today* **2005**, *107–108*, 920–925. [[CrossRef](#)]
43. Stefanidis, S.D.; Kalogiannis, K.G. In-situ upgrading of biomass pyrolysis vapors: Catalyst screening on a fixed bed reactor. *Bioresour. Technol.* **2011**, *102*, 8261–8267. [[CrossRef](#)]
44. Mochizuki, T.; Atong, D.; Chen, S.-Y.; Toba, M.; Yoshimura, Y. Effect of SiO₂ pore size on catalytic fast pyrolysis of Jatropha residues by using pyrolyzer-GC/MS. *Catal. Commun.* **2013**, *36*, 1–4. [[CrossRef](#)]
45. Lv, Y.; Qian, X.; Tu, B.; Zhao, D. Generalized synthesis of core-shell structured nano-zeolite@ordered mesoporous silica composites. *Catal. Today* **2013**, *204*, 2–7. [[CrossRef](#)]
46. Hassan, A.F.; Alafid, F.; Hrdina, R. Preparation of melamine formaldehyde/nanozeolite Y composite based on nanosilica extracted from rice husks by sol-gel method: Adsorption of lead (II) ion. *J. Sol.-Gel Sci. Technol.* **2020**, *95*, 211–222. [[CrossRef](#)]
47. Wan, Z.; Li, G.K.; Wang, C.; Yang, H.; Zhang, D. Relating coke formation and characteristics to deactivation of ZSM-5 zeolite in methanol to gasoline conversion. *Appl. Catal. A Gen.* **2018**, *549*, 141–151. [[CrossRef](#)]
48. Du, J.; Gao, L.; Yang, Y.; Chen, G.; Guo, S.; Omran, M.; Chen, J.; Ruan, R. Study on thermochemical characteristics properties and pyrolysis kinetics of the mixtures of waste corn stalk and pyrolusite. *Bioresour. Technol.* **2021**, *324*, 124660. [[CrossRef](#)]
49. Lin, X.; Zhang, Z.; Wang, Q. Evaluation of zeolite catalyst on product distribution and synergy during wood-plastic composite catalytic pyrolysis. *Energy* **2019**, *189*, 116174. [[CrossRef](#)]
50. Lazaridis, P.A.; Fotopoulos, A.P.; Karakoulia, S.A.; Triantafyllidis, K.S. Catalytic fast pyrolysis of kraft lignin with conventional, mesoporous and nanosized ZSM-5 zeolite for the production of alkyl-phenols and aromatics. *Front. Chem.* **2018**, *6*, 295. [[CrossRef](#)]

51. Hassan, N.S.; Jalil, A.A.; Hitam, C.N.C.; Vo, D.V.N.; Nabgan, W. Biofuels and renewable chemicals production by catalytic pyrolysis of cellulose: A review. *Environ. Chem. Lett.* **2020**, *18*, 1625–1648. [[CrossRef](#)]
52. Yu, Y.; Li, X.; Su, L.; Zhang, Y.; Wang, Y.; Zhang, H. The role of shape selectivity in catalytic fast pyrolysis of lignin with zeolite catalysts. *Appl. Catal. A Gen.* **2012**, *447–448*, 115–123. [[CrossRef](#)]
53. Kim, Y.-M.; Jeong, J.; Ryu, S.; Lee, H.W.; Jung, J.S.; Siddiqui, M.Z.; Jung, S.-C.; Jeon, J.-K.; Jae, J.; Park, Y.-K. Catalytic pyrolysis of wood polymer composites over hierarchical mesoporous zeolites. *Energy Convers. Manag.* **2019**, *195*, 727–737. [[CrossRef](#)]
54. Soltanian, S.; Lee, C.L.; Lam, S.S. A review on the role of hierarchical zeolites in the production of transportation fuels through catalytic fast pyrolysis of biomass. *Biofuel Res. J.* **2020**, *7*, 1217–1234. [[CrossRef](#)]
55. Qian, M.; Zhao, Y.; Huo, E.; Wang, C.; Zhang, X.; Lin, X.; Wang, L.; Kong, X.; Ruan, R.; Lei, H. Improving catalytic production of aromatic hydrocarbons with a mesoporous ZSM-5 modified with nanocellulose as a green template. *J. Anal. Appl. Pyrolysis* **2022**, *166*, 105624. [[CrossRef](#)]
56. Casoni, A.I.; Nievas, M.L.; Moyano, E.L.; Álvarez, M.; Diez, A.; Dennehy, M.; Volpe, M.A. Catalytic pyrolysis of cellulose using MCM-41 type catalysts. *Appl. Catal. A Gen.* **2016**, *514*, 235–240. [[CrossRef](#)]
57. Veloso, C.M.; Rangel, M.C. Preparação de Carbonos Porosos por Moldagem Sequencial. *Química Nova* **2009**, *32*, 2133–2141. [[CrossRef](#)]
58. Hagemann, N.; Spokas, K.; Schmidt, H.-P.; Kägi, R.; Böhler, M.A.; Bucheli, T.D. Activated carbon, biochar and charcoal: Linkages and synergies across pyrogenic carbon's ABCs. *Water* **2018**, *10*, 182. [[CrossRef](#)]
59. Da Silva, L.A.; Borges, S.M.S.; Paulino, P.N.; Fraga, M.A.; de Oliva, S.T.; Marchetti, S.G.; Rangel, M.D.C. Methylene blue oxidation over iron oxide supported on activated carbon derived from peanut hulls. *Catal. Today* **2017**, *289*, 237–248. [[CrossRef](#)]
60. Lima, S.B.; Borges, S.M.S.; Rangel, M.D.C.; Marchetti, S.G. Effect of iron content on the catalytic properties of activated carbon-supported magnetite derived from biomass. *J. Braz. Chem. Soc.* **2013**, *24*, 344–354. [[CrossRef](#)]
61. Yang, H.; Chen, Z.; Chen, W.; Chen, Y.; Wang, X.; Chen, H. Role of porous structure and active O-containing groups of activated biochar catalyst during biomass catalytic pyrolysis. *Energy* **2020**, *210*, 118646. [[CrossRef](#)]
62. Dai, L.; Zeng, Z.; Tian, X.; Jiang, L.; Yu, Z.; Wu, Q.; Wang, Y.; Liu, Y.; Ruan, R. Microwave-assisted catalytic pyrolysis of torrefied corn cob for phenol-rich bio-oil production over Fe modified bio-char catalyst. *J. Anal. Appl. Pyrolysis* **2019**, *143*, 104691. [[CrossRef](#)]
63. Liu, S.; Wu, G.; Gao, Y.; Li, B.; Feng, Y.; Zhou, J.; Hu, X.; Huang, Y.; Zhang, S.; Zhang, H. Understanding the catalytic upgrading of bio-oil from pine pyrolysis over CO₂-activated biochar. *Renew. Energy* **2021**, *174*, 538–546. [[CrossRef](#)]
64. Huo, E.; Duan, D.; Lei, H.; Liu, C.; Zhang, Y.; Wu, J.; Zhao, Y.; Huang, Z.; Qian, M.; Zhang, Q.; et al. Phenols production from Douglas fir catalytic pyrolysis with MgO and biomass-derived activated carbon catalysts. *Energy* **2020**, *199*, 117459. [[CrossRef](#)]
65. Han, T.; Ding, S.; Yang, W.; Jönsson, P. Catalytic pyrolysis of lignin using low-cost materials with different acidities and textural properties as catalysts. *Chem. Eng. J.* **2019**, *373*, 846–856. [[CrossRef](#)]
66. Rouquerol, J.; Avnir, D.; Fairbridge, C.W.; Everett, D.H.; Haynes, J.M.; Pernicone, N.; Ramsay, J.D.F.; Sing, K.S.W.; Unger, K.K. Recommendations for the characterization of porous solids (Technical Report). *Pure Appl. Chem.* **1994**, *66*, 1739–1758. [[CrossRef](#)]
67. Cao, L.; Yu, I.K.; Chen, S.S.; Tsang, D.C.; Wang, L.; Xiong, X.; Zhang, S.; Ok, Y.S.; Kwon, E.E.; Song, H.; et al. Production of 5-hydroxymethylfurfural from starch-rich food waste catalyzed by sulfonated biochar. *Bioresour. Technol.* **2018**, *252*, 76–82. [[CrossRef](#)]
68. Mahajan, A.; Gupta, P. Carbon-based solid acids: A review. *Environ. Chem. Lett.* **2020**, *18*, 299–314. [[CrossRef](#)]
69. Chen, S.S.; Maneerung, T.; Tsang, D.C.; Ok, Y.S.; Wang, C.-H. Valorization of biomass to hydroxymethylfurfural, levulinic acid, and fatty acid methyl ester by heterogeneous catalysts. *Chem. Eng. J.* **2017**, *328*, 246–273. [[CrossRef](#)]
70. Bu, Q.; Lei, H.; Wang, L.; Wei, Y.; Zhu, L.; Liu, Y.; Liang, J.; Tang, J. Renewable phenols production by catalytic microwave pyrolysis of Douglas fir sawdust pellets with activated carbon catalysts. *Bioresour. Technol.* **2013**, *142*, 546–552. [[CrossRef](#)]
71. Mamaeva, A.; Tahmasebi, A.; Tian, L.; Yu, J. Microwave-assisted catalytic pyrolysis of lignocellulosic biomass for production of phenolic-rich bio-oil. *Bioresour. Technol.* **2016**, *211*, 382–389. [[CrossRef](#)] [[PubMed](#)]
72. Omoriyekomwan, J.E.; Tahmasebi, A.; Yu, J. Production of phenol-rich bio-oil during catalytic fixed-bed and microwave pyrolysis of palm kernel shell. *Bioresour. Technol.* **2016**, *207*, 188–196. [[CrossRef](#)]
73. Ye, X.-N.; Lu, Q.; Wang, X.; Guo, H.-Q.; Cui, M.-S.; Dong, C.-Q.; Yang, Y.-P. Catalytic Fast Pyrolysis of Cellulose and Biomass to Selectively Produce Levoglucosenone Using Activated Carbon Catalyst. *ACS Sustain. Chem. Eng.* **2017**, *5*, 10815–10825. [[CrossRef](#)]
74. Chen, W.; Li, K.; Xia, M.; Yang, H.; Chen, Y.; Chen, X.; Che, Q.; Chen, H. Catalytic deoxygenation co-pyrolysis of bamboo wastes and microalgae with biochar catalyst. *Energy* **2018**, *157*, 472–482. [[CrossRef](#)]
75. Zhang, Y.; Lei, H.; Yang, Z.; Qian, K.; Villota, E. Renewable high-purity mono-phenol production from catalytic microwave-induced pyrolysis of cellulose over biomass-derived activated carbon catalyst. *ACS Sustain. Chem. Eng.* **2018**, *6*, 5349–5357. [[CrossRef](#)]
76. Chen, W.; Fang, Y.; Li, K.; Chen, Z.; Xia, M.; Gong, M.; Chen, Y.; Yang, H.; Tu, X.; Chen, H. Bamboo wastes catalytic pyrolysis with N-doped biochar catalyst for phenols products. *Appl. Energy* **2020**, *260*, 114242. [[CrossRef](#)]
77. Nejati, B.; Adami, P.; Bozorg, A.; Tavasoli, A.; Mirzahosseini, A.H. Catalytic pyrolysis and bio-products upgrading derived from *Chlorella vulgaris* over its biochar and activated biochar-supported Fe catalysts. *J. Anal. Appl. Pyrolysis* **2020**, *152*, 104799. [[CrossRef](#)]
78. Mgbemere, H.E.; Ekpe, I.C.; Lawai, G.I. Zeolite Synthesis, Characterization and Application Areas: A Review. *Int. Res. J. Environ. Sci.* **2017**, *6*, 45–59.

79. Rahman, M.M.; Liu, R.; Cai, J. Catalytic fast pyrolysis of biomass over zeolites for high quality bio-oil—A review. *Fuel Process. Technol.* **2018**, *180*, 32–46. [[CrossRef](#)]
80. Nippes, R.P.; Macruz, P.D.; Molina, L.C.A.; Scaliante, M.H.N.O. Hydroxychloroquine Adsorption in Aqueous Medium Using Clinoptilolite Zeolite. *Water Air Soil Pollut.* **2022**, *233*, 287. [[CrossRef](#)] [[PubMed](#)]
81. Usman, M. Recent Progress of SAPO-34 Zeolite Membranes for CO₂ Separation: A Review. *Membranes* **2022**, *12*, 507. [[CrossRef](#)]
82. Yoon, J.S.; Lee, T.; Choi, J.-W.; Suh, D.J.; Lee, K.; Ha, J.-M.; Choi, J. Layered MWW zeolite-supported Rh catalysts for the hydrodeoxygenation of lignin model compounds. *Catal. Today* **2017**, *293–294*, 142–150. [[CrossRef](#)]
83. Hita, I.; Cordero-Lanzac, T.; García-Mateos, F.J.; Azkoiti, M.J.; Rodríguez-Mirasol, J.; Cordero, T.; Bilbao, J. Enhanced production of phenolics and aromatics from raw bio-oil using HZSM-5 zeolite additives for PtPd/C and NiW/C catalysts. *Appl. Catal. B Environ.* **2019**, *259*, 128112. [[CrossRef](#)]
84. Vayssilov, G.N.; Rösch, N. Influence of alkali and alkaline earth cations on the Brønsted acidity of zeolites. *J. Phys. Chem. B* **2001**, *105*, 4277–4284. [[CrossRef](#)]
85. Moreno, E.; Rajagopal, K. Desafios da acidez na catálise em estado sólido. *Quím. Nova* **2009**, *32*, 538–543. [[CrossRef](#)]
86. Aho, A.; Salmi, T.; Murzin, D.Y. Catalytic Pyrolysis of Lignocellulosic Biomass. In *Production of Bio-Fuels and Bio-Chemicals*; Kostas, S.T., Angelos, A.L., Eds.; Elsevier: Amsterdam, The Netherlands, 2013; pp. 137–159. [[CrossRef](#)]
87. Ani, F.N. Utilization of bioresources as fuels and energy generation. In *Electric Renewable Energy Systems*; Elsevier: Amsterdam, The Netherlands, 2016; pp. 140–155. [[CrossRef](#)]
88. Dabros, T.M.; Stummann, M.Z.; Høj, M.; Jensen, P.A.; Grunwaldt, J.-D.; Gabrielsen, J.; Mortensen, P.M.; Jensen, A.D. Transportation fuels from biomass fast pyrolysis, catalytic hydrodeoxygenation, and catalytic fast hydrolysis. *Prog. Energy Combust. Sci.* **2018**, *68*, 268–309. [[CrossRef](#)]
89. Wang, C.; Zhang, X.; Liu, Q.; Zhang, Q.; Chen, L.; Ma, L. A review of conversion of lignocellulose biomass to liquid transport fuels by integrated refining strategies. *Fuel Process. Technol.* **2020**, *208*, 106485. [[CrossRef](#)]
90. Mayer, F.M.; Teixeira, C.M.; Pacheco, J.G.A.; de Souza, C.T.; Bauer, D.D.V.; Caramão, E.B.; Espíndola, J.D.S.; Trierweiler, J.O.; Lopez, O.W.P.; Zini, C.A. Characterization of analytical fast pyrolysis vapors of medium-density fiberboard (MDF) using metal-modified HZSM-5. *J. Anal. Appl. Pyrolysis* **2018**, *136*, 87–95. [[CrossRef](#)]
91. Jin, T.; Wang, H.; Peng, J.; Wu, Y.; Huang, Z.; Tian, X.; Ding, M. Catalytic pyrolysis of lignin with metal-modified HZSM-5 as catalysts for monocyclic aromatic hydrocarbons production. *Fuel Process. Technol.* **2022**, *230*, 107201. [[CrossRef](#)]
92. Kantarelis, E.; Javed, R.; Stefanidis, S.; Psarras, A.; Iliopoulou, E.; Lappas, A. Engineering the Catalytic Properties of HZSM5 by Cobalt Modification and Post-synthetic Hierarchical Porosity Development. *Top. Catal.* **2019**, *62*, 773–785. [[CrossRef](#)]
93. Patel, A.B.; Shaikh, S.; Jain, K.R.; Desai, C.; Madamwar, D. Polycyclic Aromatic Hydrocarbons: Sources, Toxicity, and Remediation Approaches. *Front. Microbiol.* **2020**, *11*, 1–23. [[CrossRef](#)]
94. Escola, J.; Aguado, J.; Serrano, D.; García, A.; Peral, A.; Briones, L.; Calvo, R.; Fernandez, E. Catalytic hydroreforming of the polyethylene thermal cracking oil over Ni supported hierarchical zeolites and mesostructured aluminosilicates. *Appl. Catal. B Environ.* **2011**, *106*, 405–415. [[CrossRef](#)]
95. Dai, L.; Wang, Y.; Liu, Y.; Ruan, R.; Duan, D.; Zhao, Y.; Yu, Z.; Jiang, L. Catalytic fast pyrolysis of torrefied corn cob to aromatic hydrocarbons over Ni-modified hierarchical ZSM-5 catalyst. *Bioresour. Technol.* **2019**, *272*, 407–414. [[CrossRef](#)] [[PubMed](#)]
96. Hernando, H.; Moreno, I.; Feroso, J.; Ochoa-Hernández, C.; Pizarro, P.; Coronado, J.M.; Čejka, J.; Serrano, D.P. Biomass catalytic fast pyrolysis over hierarchical ZSM-5 and Beta zeolites modified with Mg and Zn oxides. *Biomass Convers. Biorefinery* **2017**, *7*, 289–304. [[CrossRef](#)]
97. Ryu, H.W.; Lee, H.W.; Jae, J.; Park, Y.-K. Catalytic pyrolysis of lignin for the production of aromatic hydrocarbons: Effect of magnesium oxide catalyst. *Energy* **2019**, *179*, 669–675. [[CrossRef](#)]
98. Hernando, H.; Jiménez-Sánchez, S.; Feroso, J.; Pizarro, P.; Coronado, J.M.; Serrano, D.P. Assessing biomass catalytic pyrolysis in terms of deoxygenation pathways and energy yields for the efficient production of advanced biofuels. *Catal. Sci. Technol.* **2016**, *6*, 2829–2843. [[CrossRef](#)]
99. Ding, K.; Zhong, Z.; Wang, J.; Zhang, B.; Fan, L.; Liu, S.; Wang, Y.; Liu, Y.; Zhong, D.; Chen, P.; et al. Improving hydrocarbon yield from catalytic fast co-pyrolysis of hemicellulose and plastic in the dual-catalyst bed of CaO and HZSM-5. *Bioresour. Technol.* **2018**, *261*, 86–92. [[CrossRef](#)] [[PubMed](#)]
100. Liu, C.; Wang, H.; Karim, A.M.; Sun, J.; Wang, Y. Catalytic fast pyrolysis of lignocellulosic biomass. *Chem. Soc. Rev.* **2014**, *43*, 7594–7623. [[CrossRef](#)]
101. Hu, B.; Zhang, Z.-X.; Xie, W.-L.; Liu, J.; Li, Y.; Zhang, W.-M.; Fu, H.; Lu, Q. Advances on the fast pyrolysis of biomass for the selective preparation of phenolic compounds. *Fuel Process. Technol.* **2022**, *237*, 107465. [[CrossRef](#)]
102. Sharifzadeh, M.; Sadeqzadeh, M.; Guo, M.; Borhani, T.N.; Konda, N.M.; Garcia, M.C.; Wang, L.; Hallett, J.; Shah, N. The multi-scale challenges of biomass fast pyrolysis and bio-oil upgrading: Review of the state of art and future research directions. *Prog. Energy Combust. Sci.* **2019**, *71*, 1–80. [[CrossRef](#)]
103. Chen, X.; Chen, Y.; Yang, H.; Wang, X.; Che, Q.; Chen, W.; Chen, H. Catalytic fast pyrolysis of biomass: Selective deoxygenation to balance the quality and yield of bio-oil. *Bioresour. Technol.* **2019**, *273*, 153–158. [[CrossRef](#)] [[PubMed](#)]
104. Kumar, R.; Strezov, V.; Lovell, E.; Kan, T.; Weldekidan, H.; He, J.; Jahan, S.; Dastjerdi, B.; Scott, J. Enhanced bio-oil deoxygenation activity by Cu/zeolite and Ni/zeolite catalysts in combined in-situ and ex-situ biomass pyrolysis. *J. Anal. Appl. Pyrolysis* **2019**, *140*, 148–160. [[CrossRef](#)]

105. Zhang, J.; Gu, J.; Yuan, H.; Chen, Y. Catalytic fast pyrolysis of waste mixed cloth for the production of value-added chemicals. *Waste Manag.* **2021**, *127*, 141–146. [[CrossRef](#)]
106. Chong, Y.Y.; Thangalazhy-Gopakumar, S.; Ng, H.K.; Lee, L.Y.; Gan, S. Effect of oxide catalysts on the properties of bio-oil from in-situ catalytic pyrolysis of palm empty fruit bunch fiber. *J. Environ. Manag.* **2019**, *247*, 38–45. [[CrossRef](#)]
107. Chireshe, F.; Collard, F.-X.; Görgens, J.F. Production of an upgraded bio-oil with minimal water content by catalytic pyrolysis: Optimisation and comparison of CaO and MgO performances. *J. Anal. Appl. Pyrolysis* **2020**, *146*, 104751. [[CrossRef](#)]
108. Gupta, J.; Papadikis, K.; Konyshcheva, E.Y.; Lin, Y.; Kozhevnikov, I.V.; Li, J. CaO catalyst for multi-route conversion of oakwood biomass to value-added chemicals and fuel precursors in fast pyrolysis. *Appl. Catal. B Environ.* **2021**, *285*, 119858. [[CrossRef](#)]
109. Raymundo, L.M.; Mullen, C.A.; Boateng, A.A.; DeSisto, W.J.; Trierweiler, J.O. Production of partially deoxygenated pyrolysis oil from switchgrass via Ca(OH)₂, CaO, and Ca(COOH)₂ cofeeding. *Energy Fuels* **2020**, *34*, 12616–12625. [[CrossRef](#)]
110. Lin, X.; Zhang, Z.; Zhang, Z.; Sun, J.; Wang, Q.; Pittman, C.U. Catalytic fast pyrolysis of a wood-plastic composite with metal oxides as catalysts. *Waste Manag.* **2018**, *79*, 38–47. [[CrossRef](#)]
111. Shao, S.; Liu, C.; Xiang, X.; Li, X.; Zhang, H.; Xiao, R.; Cai, Y. In situ catalytic fast pyrolysis over CeO₂ catalyst: Impact of biomass source, pyrolysis temperature and metal ion. *Renew. Energy* **2021**, *177*, 1372–1381. [[CrossRef](#)]
112. Li, Y.; Hu, B.; Fu, H.; Zhang, Z.-X.; Guo, Z.-T.; Zhou, G.-Z.; Zhu, L.-J.; Liu, J.; Lu, Q. Fast pyrolysis of bagasse catalyzed by mixed alkaline-earth metal oxides for the selective production of 4-vinylphenol. *J. Anal. Appl. Pyrolysis* **2022**, *164*, 105531. [[CrossRef](#)]
113. Veses, A.; Aznar, M.; Martínez, I.; Martínez, J.; López, J.; Navarro, M.; Callén, M.; Murillo, R.; García, T. Catalytic pyrolysis of wood biomass in an auger reactor using calcium-based catalysts. *Bioresour. Technol.* **2014**, *162*, 250–258. [[CrossRef](#)]
114. Locatell, W.d.R.; Laurenti, D.; Schuurman, Y.; Guilhaume, N. Ex-situ catalytic upgrading of pyrolysis vapors using mixed metal oxides. *J. Anal. Appl. Pyrolysis* **2021**, *158*, 105241. [[CrossRef](#)]
115. Vichaphund, S.; Sricharoenchaikul, V.; Aton, D. Industrial waste derived CaO-based catalysts for upgrading volatiles during pyrolysis of Jatropha residues. *J. Anal. Appl. Pyrolysis* **2017**, *124*, 568–575. [[CrossRef](#)]
116. Jiang, H.; Liu, B.; Chen, J.; Hong, W.; Zhang, Y.; Liu, H. Comparative investigation on the effects of formate salt additives on pyrolysis characteristics of corn straw. *J. Anal. Appl. Pyrolysis* **2022**, *162*, 105450. [[CrossRef](#)]
117. Xia, S.; Yang, H.; Lei, S.; Lu, W.; Cai, N.; Xiao, H.; Chen, Y.; Chen, H. Iron salt catalytic pyrolysis of biomass: Influence of iron salt type. *Energy* **2023**, *262*, 125415. [[CrossRef](#)]
118. Eibner, S.; Broust, F.; Blin, J.; Julbe, A. Catalytic effect of metal nitrate salts during pyrolysis of impregnated biomass. *J. Anal. Appl. Pyrolysis* **2015**, *113*, 143–152. [[CrossRef](#)]
119. Carvalho, W.S.; Cunha, I.F.; Pereira, M.S.; Ataíde, C.H. Thermal decomposition profile and product selectivity of analytical pyrolysis of sweet sorghum bagasse. Effect of addition of inorganic salts. *Ind. Crops Prod.* **2015**, *74*, 372–380. [[CrossRef](#)]
120. Li, H.; Wang, Y.; Zhou, N.; Dai, L.; Deng, W.; Liu, C.; Cheng, Y.; Liu, Y.; Cobb, K.; Chen, P.; et al. Applications of calcium oxide-based catalysts in biomass pyrolysis/gasification—A review. *J. Clean. Prod.* **2021**, *291*, 125826. [[CrossRef](#)]
121. Cao, Z.; Niu, J.; Gu, Y.; Zhang, R.; Liu, Y.; Luo, L. Catalytic pyrolysis of rice straw: Screening of various metal salts, metal basic oxides, acidic metal oxide and zeolite catalyst on products yield and characterization. *J. Clean. Prod.* **2020**, *269*, 122079. [[CrossRef](#)]
122. Sun, L.; Zhang, X.; Chen, L.; Zhao, B.; Yang, S.; Xie, X. Effects of Fe contents on fast pyrolysis of biomass with Fe/CaO catalysts. *J. Anal. Appl. Pyrolysis* **2016**, *119*, 133–138. [[CrossRef](#)]
123. Rahman, M.; Nishu; Sarker, M.; Chai, M.; Li, C.; Liu, R.; Cai, J. Potentiality of combined catalyst for high quality bio-oil production from catalytic pyrolysis of pinewood using an analytical Py-GC/MS and fixed bed reactor. *J. Energy Inst.* **2020**, *93*, 1737–1746. [[CrossRef](#)]
124. Zhang, C.; Hu, X.; Guo, H.; Wei, T.; Dong, D.; Hu, G.; Hu, S.; Xiang, J.; Liu, Q.; Wang, Y. Pyrolysis of poplar, cellulose and lignin: Effects of acidity and alkalinity of the metal oxide catalysts. *J. Anal. Appl. Pyrolysis* **2018**, *134*, 590–605. [[CrossRef](#)]
125. Li, C.; Zhang, J.; Gu, J.; Yuan, H.; Chen, Y. Insight into the role of varied acid-base sites on fast pyrolysis kinetics and mechanism of cellulose. *Waste Manag.* **2021**, *135*, 140–149. [[CrossRef](#)]
126. Chen, X.; Chen, Y.; Yang, H.; Chen, W.; Wang, X.; Chen, H. Fast pyrolysis of cotton stalk biomass using calcium oxide. *Bioresour. Technol.* **2017**, *233*, 15–20. [[CrossRef](#)] [[PubMed](#)]
127. Zhang, H.; Lyu, G.; Zhang, A.; Li, X.; Xie, J. Effects of ferric chloride pretreatment and surfactants on the sugar production from sugarcane bagasse. *Bioresour. Technol.* **2018**, *265*, 93–101. [[CrossRef](#)] [[PubMed](#)]
128. Loow, Y.-L.; Wu, T.Y.; Lim, Y.S.; Tan, K.A.; Siow, L.F.; Jahim, J.M.; Mohammad, A.W. Improvement of xylose recovery from the stalks of oil palm fronds using inorganic salt and oxidative agent. *Energy Convers. Manag.* **2017**, *138*, 248–260. [[CrossRef](#)]
129. Shafeeyan, M.S.; Daud, W.M.A.W.; Houshmand, A.; Shamiri, A.A. review on surface modification of activated carbon for carbon dioxide adsorption. *J. Anal. Appl. Pyrolysis* **2010**, *89*, 143–151. [[CrossRef](#)]
130. Badosz, T.J.; Ania, C.O. Surface chemistry of activated carbons and its characterization. *Interface Sci. Technol.* **2006**, *7*, 159–229.
131. Salame, I.I.; Badosz, T.J. Role of surface chemistry in adsorption of phenol on activated carbons. *J. Colloid Interface Sci.* **2003**, *264*, 307–312. [[CrossRef](#)]
132. Pradhan, B.K.; Sandle, N.K. Effect of different oxidizing agent treatments on the surface properties of activated carbons. *Carbon* **1999**, *37*, 1323–1332. [[CrossRef](#)]
133. Lee, H.; Kim, H.; Yu, M.J.; Ko, C.H.; Jeon, J.-K.; Jae, J.; Park, S.H.; Jung, S.-C.; Park, Y.-K. Catalytic Hydrodeoxygenation of Bio-oil Model Compounds over Pt/HY Catalyst. *Sci. Rep.* **2016**, *6*, 28765. [[CrossRef](#)]

134. Vichaphund, S.; Aht-Ong, D.; Sricharoenchaikul, V.; Atong, D. Production of aromatic compounds from catalytic fast pyrolysis of Jatropha residues using metal/HZSM-5 prepared by ion-exchange and impregnation methods. *Renew. Energy* **2015**, *79*, 28–37. [[CrossRef](#)]
135. Stummann, M.Z.; Elevera, E.; Hansen, A.B.; Hansen, L.P.; Beato, P.; Davidsen, B.; Wiwel, P.; Gabrielsen, J.; Jensen, P.A.; Jensen, A.D.; et al. Catalytic hydropyrolysis of biomass using supported CoMo catalysts—Effect of metal loading and support acidity. *Fuel* **2020**, *264*, 116867. [[CrossRef](#)]
136. Li, P.; Li, D.; Yang, H.; Wang, X.; Chen, H. Effects of Fe-, Zr-, and Co-Modified Zeolites and Pretreatments on Catalytic Upgrading of Biomass Fast Pyrolysis Vapors. *Energy Fuels* **2016**, *30*, 3004–3013. [[CrossRef](#)]
137. Zhang, S.; Zhang, H.; Liu, X.; Zhu, S.; Hu, L.; Zhang, Q. Upgrading of bio-oil from catalytic pyrolysis of pretreated rice husk over Fe-modified ZSM-5 zeolite catalyst. *Fuel Process. Technol.* **2018**, *175*, 17–25. [[CrossRef](#)]
138. Dai, G.; Wang, S.; Zou, Q.; Huang, S. Improvement of aromatics production from catalytic pyrolysis of cellulose over metal-modified hierarchical HZSM-5. *Fuel Process. Technol.* **2018**, *179*, 319–323. [[CrossRef](#)]
139. Kumar, R.; Strezov, V.; Lovell, E.; Kan, T.; Weldekidan, H.; He, J.; Dastjerdi, B.; Scott, J. Bio-oil upgrading with catalytic pyrolysis of biomass using Copper/zeolite-Nickel/zeolite and Copper-Nickel/zeolite catalysts. *Bioresour. Technol.* **2019**, *279*, 404–409. [[CrossRef](#)] [[PubMed](#)]
140. Kumar, R.; Strezov, V.; Kan, T.; Weldekidan, H.; He, J.; Jahan, S. Investigating the Effect of Mono- And Bimetallic/Zeolite Catalysts on Hydrocarbon Production during Bio-oil Upgrading from Ex Situ Pyrolysis of Biomass. *Energy Fuels* **2019**, *34*, 389–400. [[CrossRef](#)]
141. Zheng, Y.; Wang, J.; Li, D.; Liu, C.; Lu, Y.; Lin, X.; Zheng, Z. Activity and selectivity of Ni–Cu bimetallic zeolites catalysts on biomass conversion for bio-aromatic and bio-phenols. *J. Energy Inst.* **2021**, *97*, 57–72. [[CrossRef](#)]
142. Xue, S.; Luo, Z.; Zhou, Q.; Sun, H.; Du, L. Regulation mechanism of three key parameters on catalytic characterization of molybdenum modified bimetallic micro-mesoporous catalysts during catalytic fast pyrolysis of enzymatic hydrolysis lignin. *Bioresour. Technol.* **2021**, *337*, 125396. [[CrossRef](#)] [[PubMed](#)]
143. Zhu, L.; Hu, Z.; Huang, M.; Peng, H.; Zhang, W.; Chen, D.; Ma, Z. Valorisation of cotton stalk toward bio-aromatics: Effect of wet torrefaction deoxygenation and demineralization pretreatment on catalytic fast pyrolysis using Ga modified hierarchical zeolite. *Fuel* **2022**, *330*, 125571. [[CrossRef](#)]
144. Shao, J.; Jiang, H.; Yang, M.; Xiao, J.; Yang, H.; Chen, Y.; Zhang, S.; Chen, H. Catalytic fast pyrolysis of cellulose over different metal-modified ZSM-5 zeolites for light olefins. *J. Anal. Appl. Pyrolysis* **2022**, *166*, 105628. [[CrossRef](#)]
145. Huang, M.; Xu, J.; Ma, Z.; Yang, Y.; Zhou, B.; Wu, C.; Ye, J.; Zhao, C.; Liu, X.; Chen, D.; et al. Bio-BTX production from the shape selective catalytic fast pyrolysis of lignin using different zeolite catalysts: Relevance between the chemical structure and the yield of bio-BTX. *Fuel Process. Technol.* **2021**, *216*, 106792. [[CrossRef](#)]
146. Lv, P.; Yan, L.; Liu, Y.; Wang, M.; Bao, W.; Li, F. Catalytic conversion of coal pyrolysis vapors to light aromatics over hierarchical Y-type zeolites. *J. Energy Inst.* **2020**, *93*, 1354–1363. [[CrossRef](#)]
147. Wei, B.; Jin, L.; Wang, D.; Shi, H.; Hu, H. Catalytic upgrading of lignite pyrolysis volatiles over modified HY zeolites. *Fuel* **2020**, *259*, 116234. [[CrossRef](#)]
148. Osei, G.K.; Nzihou, A.; Yaya, A.; Minh, D.P.; Onwona-Agyeman, B. Catalytic Pyrolysis of Waste Engine Oil over Y Zeolite Synthesized from Natural Clay. *Waste Biomass Valorization* **2021**, *12*, 4157–4170. [[CrossRef](#)]
149. Paysepar, H.; Rao, K.T.V.; Yuan, Z.; Shui, H.; Xu, C. Improving activity of ZSM-5 zeolite catalyst for the production of monomeric aromatics/phenolics from hydrolysis lignin via catalytic fast pyrolysis. *Appl. Catal. A Gen.* **2018**, *563*, 154–162. [[CrossRef](#)]
150. Sun, L.; Zhang, X.; Chen, L.; Zhao, B.; Yang, S.; Xie, X. Comparison of catalytic fast pyrolysis of biomass to aromatic hydrocarbons over ZSM-5 and Fe/ZSM-5 catalysts. *J. Anal. Appl. Pyrolysis* **2016**, *121*, 342–346. [[CrossRef](#)]
151. Dada, T.K.; Islam, A.; Duan, A.X.; Antunes, E. Catalytic co-pyrolysis of ironbark and waste cooking oil using X-strontium/Y-zeolite (X = Ni, Cu, Zn, Ag, and Fe). *J. Energy Inst.* **2022**, *104*, 89–97. [[CrossRef](#)]
152. Robinson, A.M.; Hensley, J.E.; Medlin, J.W. Bifunctional Catalysts for Upgrading of Biomass-Derived Oxygenates: A Review. *Catalysis* **2022**, *6*, 5026–5043. [[CrossRef](#)]
153. Zhang, X.; Sun, L.; Chen, L.; Xie, X.; Zhao, B.; Si, H.; Meng, G. Comparison of catalytic upgrading of biomass fast pyrolysis vapors over CaO and Fe(III)/CaO catalysts. *J. Anal. Appl. Pyrolysis* **2014**, *108*, 35–40. [[CrossRef](#)]
154. Kantarelis, E.; Yang, W.; Blasiak, W. Effects of Silica-Supported Nickel and Vanadium on Liquid Products of Catalytic Steam Pyrolysis of Biomass. *Energy Fuels* **2014**, *28*, 591–599. [[CrossRef](#)]
155. Shahabuddin, M.; Krishna, B.B.; Bhaskar, T.; Perkins, G. Advances in the thermo-chemical production of hydrogen from biomass and residual wastes: Summary of recent techno-economic analyses. *Bioresour. Technol.* **2020**, *299*, 122557. [[CrossRef](#)]
156. Feroso, J.; Hernando, H.; Jana, P.; Moreno, I.; Přeč, J.; Ochoa-Hernández, C.; Pizarro, P.; Coronado, J.M.; Čejka, J.; Serrano, D.P. Lamellar and pillared ZSM-5 zeolites modified with MgO and ZnO for catalytic fast-pyrolysis of eucalyptus woodchips. *Catal. Today* **2016**, *277*, 171–181. [[CrossRef](#)]
157. Liu, S.; Zhang, Y.; Fan, L.; Zhou, N.; Tian, G.; Zhu, X.; Cheng, Y.; Wang, Y.; Liu, Y.; Chen, P.; et al. Bio-oil production from sequential two-step catalytic fast microwave-assisted biomass pyrolysis. *Fuel* **2017**, *196*, 261–268. [[CrossRef](#)]
158. Naqvi, S.R.; Uemura, Y.; Yusup, S.B. Catalytic pyrolysis of paddy husk in a drop type pyrolyzer for bio-oil production: The role of temperature and catalyst. *J. Anal. Appl. Pyrolysis* **2014**, *106*, 57–62. [[CrossRef](#)]

159. Zhou, L.; Yang, H.; Wu, H.; Wang, M.; Cheng, D. Catalytic pyrolysis of rice husk by mixing with zinc oxide: Characterization of bio-oil and its rheological behavior. *Fuel Process. Technol.* **2013**, *106*, 385–391. [[CrossRef](#)]
160. Veses, A.; Aznar, M.; López, J.; Callén, M.; Murillo, R.; García, T. Production of upgraded bio-oils by biomass catalytic pyrolysis in an auger reactor using low cost materials. *Fuel* **2015**, *141*, 17–22. [[CrossRef](#)]
161. Dai, L.; Fan, L.; Duan, D.; Ruan, R.; Wang, Y.; Liu, Y.; Zhou, Y.; Yu, Z.; Liu, Y.; Jiang, L. Production of hydrocarbon-rich bio-oil from soapstock via fast microwave-assisted catalytic pyrolysis. *J. Anal. Appl. Pyrolysis* **2017**, *125*, 356–362. [[CrossRef](#)]
162. Abnisa, F.; Alaba, P. Recovery of liquid fuel from fossil-based solid wastes via pyrolysis technique: A review. *J. Environ. Chem. Eng.* **2021**, *9*, 106593. [[CrossRef](#)]
163. Zheng, Y.; Tao, L.; Yang, X.; Huang, Y.; Liu, C.; Zheng, Z. Study of the thermal behavior, kinetics, and product characterization of biomass and low-density polyethylene co-pyrolysis by thermogravimetric analysis and pyrolysis-GC/MS. *J. Anal. Appl. Pyrolysis* **2018**, *133*, 185–197. [[CrossRef](#)]
164. Yang, J.; Rizkiana, J.; Widayatno, W.B.; Karnjanakom, S.; Kaewpanha, M.; Hao, X.; Abudula, A.; Guan, G. Fast co-pyrolysis of low density polyethylene and biomass residue for oil production. *Energy Convers. Manag.* **2016**, *120*, 422–429. [[CrossRef](#)]
165. Rahman, H.; Bhoi, P.R.; Saha, A.; Patil, V.; Adhikari, S. Thermo-catalytic co-pyrolysis of biomass and high-density polyethylene for improving the yield and quality of pyrolysis liquid. *Energy* **2021**, *225*, 120231. [[CrossRef](#)]
166. Hassan, H.; Hameed, B.; Lim, J. Co-pyrolysis of sugarcane bagasse and waste high-density polyethylene: Synergistic effect and product distributions. *Energy* **2020**, *191*, 116545. [[CrossRef](#)]
167. Izzatie, N.; Basha, M.H.; Uemura, Y.; Hashim, M.S.M.; Amin, N.A.M.; Hamid, M.F. Co-pyrolysis of rice straw and Polyethylene Terephthalate (PET) using a fixed bed drop type pyrolyzer. *J. Phys. Conf. Ser.* **2017**, *908*, 012073. [[CrossRef](#)]
168. Çepeliogullar, Ö.; Pütün, A. A pyrolysis study for the thermal and kinetic characteristic of an agricultural waste with two different plastic wastes. *Waste Manag. Res.* **2014**, *32*, 971–979. [[CrossRef](#)]
169. Abnisa, F.; Daud, W.W.; Ramalingam, S.; Azemi, M.N.B.M.; Sahu, J. Co-pyrolysis of palm shell and polystyrene waste mixtures to synthesis liquid fuel. *Fuel* **2013**, *108*, 311–318. [[CrossRef](#)]
170. Stančin, H.; Šafář, M.; Růžičková, J.; Mikulčić, H.; Raclavská, H.; Wang, X.; Duić, N. Co-pyrolysis and synergistic effect analysis of biomass sawdust and polystyrene mixtures for production of high-quality bio-oils. *Process Saf. Environ. Prot.* **2021**, *145*, 1–11. [[CrossRef](#)]
171. Yuan, R.; Yafei, S. Catalytic pyrolysis of biomass-plastic wastes in the presence of MgO and MgCO₃ for hydrocarbon-rich oils production. *Bioresour. Technol.* **2019**, *293*, 122076. [[CrossRef](#)] [[PubMed](#)]
172. López-Uriónabarrenechea, A.; de Marco, I. Catalytic stepwise pyrolysis of packaging plastic waste. *J. Anal. Appl. Pyrolysis* **2012**, *96*, 54–62. [[CrossRef](#)]

Disclaimer/Publisher’s Note: The statements, opinions and data contained in all publications are solely those of the individual author(s) and contributor(s) and not of MDPI and/or the editor(s). MDPI and/or the editor(s) disclaim responsibility for any injury to people or property resulting from any ideas, methods, instructions or products referred to in the content.